

Quantum liquids resulted from the models with four-fermion interaction

S. V. Molodtsov*

Joint Institute for Nuclear Research, Dubna, Moscow region, RUSSIA

G. M. Zinovjev

Bogolyubov Institute for Theoretical Physics, National Academy of Sciences of Ukraine, Kiev, UKRAINE

(Dated: January 2, 2022)

A (nearly) perfect liquid discovered in the experiments with ultrarelativistic heavy ion collisions is investigated by studying the quark ensembles with four-fermion interaction as a fundamental theoretical approach. The comparative analysis of several quantum liquid models is performed and it results in the conclusion that the presence of gas–liquid phase transition is their characteristic feature. The problem of instability of small quark number droplets is discussed and argued it is rooted in the chiral soliton formation. An existence of mixed phase of the vacuum and baryon matter is proposed as a possible reason of the latter stability.

PACS numbers: 11.10.-z, 11.15.Tk

Huge amount of data on relativistic heavy ion collisions obtained recently (perceptibly before the LHC began operating) in various experiments (first of all, at RHIC), were well understood and described in terms of concepts based on the equations of relativistic hydrodynamics [1]. In particular, nearly ideal hydrodynamics, supplemented as needed by a variety of hadronic cascade models so as to correctly take into account a hadronic stage of the collision [2], quite successfully predicted an appearance of the radial and elliptic flows, their dependence on the mass, centrality, beam energy, and transverse momentum (though restricted in the magnitude), clearly indicating at the same time that the expanding liquid exhibits sufficiently specific transport properties. It is very much close to the ideal one, since the ratio η/s of its shear viscosity coefficient η to the density entropy s turned out to be a small quantity.

At this point, it should be mentioned that the exploitation of such hydrodynamic notions dates back to the early fifties of the last century when L. D. Landau had developed the model of multiple particle production in collisions of hadrons and nuclei guided by the hydrodynamics in describing the evolution of nuclear matter that occurs right upon squeezing the latter at the collision point [3]. Conceptually, this breakthrough idea had not been particularly successful in applications then because the nuclear matter had turned out to be a not very “suitable” liquid (as it was considered at the time), as the mean free path of nucleons in a produced system was fully comparable with the size of the latter.

A new generation of experiments carried out at much higher energies (reached at the LHC) quite remarkably confirmed predictions obtained by applying the past hydrodynamic ideas, rendering some of the latter, for instance, an observation of higher harmonics of flow in-

duced by the fluctuations of original geometry, or a jet quenching effect initiated by heavy and light quarks, to be not only reliable experimental data [4], but also observations that bear a profound heuristic meaning.

The physics of ultrarelativistic heavy ion collisions needs to be described, at least, at the initial stage, in the language of quantum chromodynamics (QCD) for a strongly interacting system that is in a state far from equilibrium. At the same time, the data obtained by all three LHC collaborations, while being successfully described in terms of hydrodynamics, suggest a very fast thermalization, i.e., sufficient degree of local equilibrium or, rather, isotropization, since the equations of hydrodynamics do not include the temperature of produced matter with explicit collective properties, whose theoretical explanation at the macroscopic level is still far from to be clear. In recent years, there have appeared several scenarios of what could be the dynamics of a system transiting from the initial collision state to that when it becomes (almost) equilibrium [5]. However, this problem is not discussed in the present paper. Instead, we focus on another aspect of the problem, namely, the smallness of the ratio η/s which corresponds to the presence of the strong interaction in a produced system or, in other words, small mean free path of its constituents, and try to understand the very nature of such interactions in a system, whose dynamics is governed by the coupling constant, which is likely not too large (at the LHC energies the running coupling constant in QCD as $\alpha_s \sim 0.3$ – 0.4) avoiding AdS/CFT duality (holographic QCD) arguments very popular at the moment [6].

Recently, such multiparticle (fermionic) systems are being intensively studied, particularly after they have successfully been realized in experiments as ultracold gas of fermionic atoms [7]. This (unitary) Fermi-gas is a dilute system with short-range interaction, in which the s -wave scattering among fermions saturates a unitary limit for the cross section. Such a system is naturally characterized by the absence of any internal scale (conformality) and does not depend on the details of interaction. On the

*Also at Institute of Theoretical and Experimental Physics, Moscow, RUSSIA

other hand, the interaction in such a system needs to be described non-perturbatively, since no small parameter exists in the problem. An ideal liquid observed in heavy ion experiments is exactly another remarkable example of such a strongly correlated fermionic system. An assumption, that there exists the lower bound for the ratio η/s of such fermionic systems formulated in [8], has triggered even greater interest in their study after it has been shown that η/s for the systems produced in heavy ion collisions and ultracold atomic gases turns out to be very small and close to each other in magnitude. It is interesting that the same value of that ratio is also predicted for low-energy electrons in graphene monolayers [9]. The nature of these phenomena is, however, unclear which is seen from the behavior of, say, volume viscosity that for the quark–gluon systems turns out to be nonzero and can under certain circumstances (nearby phase transitions) be a significant source of dissipation, whereas for the unitary Fermi-gases it vanishes, just as a consequence of the scale invariance.

The four-fermion (QCD-like) field theories still remain a most reliable source of quantitative information in the studies of the transport properties of strongly correlated systems and their thermodynamics, in particular, a chiral phase transition between massive hadrons and almost massless quarks. It is a thermodynamics that provides us with some general framework which lets one to understand how the properties of macroscopic matter and, in particular, its collective behavior, emerge from the laws that govern microscopic dynamics. The results of this work allows us to suppose with a sufficient, in our view, level of argumentation that the picture based on a complex collective behavior of quarks (antiquarks, gluons), which is expressed in the presence of vacuum condensates even under normal conditions, can be set by the nontrivial thermodynamic properties of vacuum, which eventually determine the observable properties of strongly interacting matter. In our opinion, this possibility was not sufficiently widely discussed and, even more so, used already at the initial stage of studies of the quark–gluon matter due to purely accidental circumstances. (As recent discussions of one of us (G.M.Z.) with E. Shuryak that have taken place during "Quark Matter 2012" have shown, similar thoughts are fully shared by him and, presumably, have occurred to him a bit earlier (see, for example, [10].)

I. THERMODYNAMICS OF THE ENSEMBLE

In the present work we consider some aspects of thermodynamical description of the quark ensemble with four-fermion interaction (generated, as it is believed, by strong stochastic gluon field) Hamiltonian density

$$\mathcal{H} = -\bar{q} (i\boldsymbol{\gamma}\nabla + m) q - j_\mu^a \int d\mathbf{y} \langle A_\mu^a A_\nu^{b'} \rangle j_\nu^{b'}, \quad (1)$$

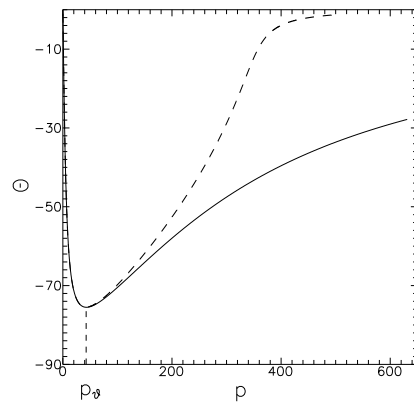


FIG. 1: The most stable equilibrium angles θ (in degrees) as function of momentum p in MeV. The solid line for NJL model, dashed one corresponds to the KKB model.

where $j_\mu^a = \bar{q} t^a \gamma_\mu q$ is the quark current, with corresponding quark operators q, \bar{q} , taken in spatial point \mathbf{x} (the variables with prime corresponds to the \mathbf{y} point), m is the current quark mass, $t^a = \lambda^a/2$ is the color gauge group $SU(N_c)$ generators, $\mu, \nu = 0, 1, 2, 3$. We take the gluon field correlator $\langle A_\mu^a A_\nu^{b'} \rangle$ in a simple form of color singlet, with contact (in time) interaction (without retarding)[29]

$$\langle A_\mu^a A_\nu^{b'} \rangle = G \delta^{ab} \delta_{\mu\nu} F(\mathbf{x} - \mathbf{y}), \quad (2)$$

(we do not include corresponding delta-function on time in this formula). This simple correlation function is a fragment of corresponding ordered exponent and besides the four-fermion interaction accompanied infinite number of multi-fermion vertices arises. But for our purposes here it would be quite enough restrict ourself with this simple form. The mentioned above effective interactions appear in natural way by the coarse-grained description of the system with handling the corresponding averaging procedure, and having in mind that vacuum gluon field changed stochastically (for example, in the form of instanton liquid, see [11]). But this elaboration of effective Hamiltonian resulting from the first principles of quantum chromodynamics (QCD) will be unessential for us, as it will be demonstrated below. The choice of correlation function in the simplest form with instantaneous interaction does not generate any problem at transforming final results from the Minkovski space to the Euclidean one and the formfactor $F(\mathbf{x})$ is interpreted in a simple way as an interaction 'potential' of point-like particles. The correlation function itself looks, formally, like a gauge non-invariant object[30]. Nevertheless, there exists an effective way to significantly compensate for this shortcoming, if all similar 'potentials' are looked through, in some sense, (to be elucidated below). For example, this set would be quite perceptible, if it becomes possible to confront two limits opposite in physics, for example, started from the formfactor with a delta-like function in the coordinate space (the Nambu–Jona-Lasinio (NJL) model [12], the correlation length is finite in this case)

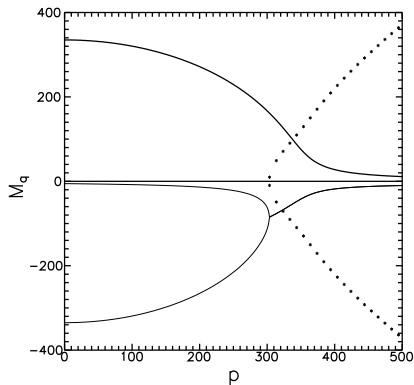


FIG. 2: Three branches of solutions for dynamical quark mass (in MeV) for the KKB model as a function of momentum (MeV). The imaginary parts of the solutions are shown by dots.

and extended to the formfactor of a delta-like function in the momentum space (clearly, the correlation length tends to infinity in this case) analogous to that is well-known in condensed matter physics as the Keldysh model (KKB) [13]. It is worth to remark here that we will need only one of its properties, although [31] of exceptional importance, which is related to the fact that, due to the special formfactor behavior, all the momentum integrations in the problem get factorized and effectively the problem becomes one-dimensional (then only integration over energy are in play). From this point of view, other models with an arbitrary formfactor (including the NJL model) could be represented as a superposition of elementary blocks obtained by using the KKB model. The utmost distributions mentioned above can be considered as a limiting case for the corresponding Gaussian correlators in the coordinate and momentum spaces, which, of course, look more realistic. The coupling constant scale G , that will turn out to be interesting for applications can be tuned by using corresponding PDG meson observables. Comparing the results obtained (by continuity arguments) one can make some conclusions about behavior of the system with practically any interaction potential.

We consider necessary to comment briefly on a case with a linear potential, which was always giving hope to discover an unusual feature in quark behavior thereby shedding some light on the nature of confinement. Meanwhile, at present however, it appears that such a singular 'potential' is even superfluous for our purposes, since the properties, we are interested in, are already revealed in the KKB model, which, in a sense, is like half way from the NJL model to that with a linear potential. Secondly, the quasiparticles in the model with a linearly increasing potential can not basically be distinguished from those in, for example, the NJL model, provided an integrable infrared singularity in the former is eliminated. As a result the same massive objects appear without the anomalies in the energy spectrum. Additionally, the analysis shows that the multi-fermion contributions present in the prob-

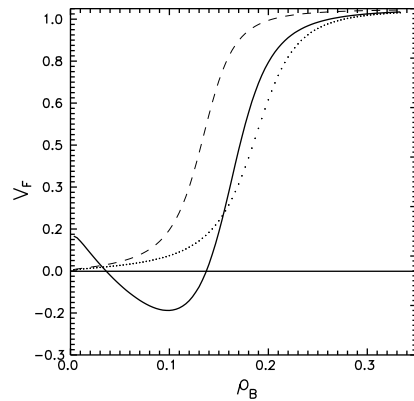


FIG. 3: The group velocity of quasiparticles v_F on the Fermi surface. The solid line describes the NJL model, the dashed one corresponds to the KKB model, the dots show the data for the KKB model tuned to the π -meson energy Figs.4–8).

lem in a general case can be reduced to the four-fermion interaction in an acceptable way by inserting the respective vacuum expectation values. In other words, even the Hamiltonian of the form (1) seems to capture the essential features of quark interactions.

It is believed that at sufficiently large interaction the ground state of the system transforms from a trivial vacuum $|0\rangle$ (the vacuum of free Hamiltonian) to the mixed state (with quark–anti-quark pairs with the opposite momenta and vacuum quantum numbers) which is presented as the Bogolyubov trial function (in that way some separate reference frame is introduced and a chiral phase becomes fixed)

$$|\sigma\rangle = \mathcal{T}|0\rangle, \quad \mathcal{T} = \prod_{p,s} \exp[\varphi_p (a_{p,s}^+ b_{-p,s}^+ + a_{p,s} b_{-p,s})].$$

Here a^+ , a and b^+ , b are the quarks creation and annihilation operators, $a|0\rangle = 0$, $b|0\rangle = 0$. The dressing transformation \mathcal{T} transmutes the quark operators to the creation and annihilation operators of quasiparticles $A = \mathcal{T} a \mathcal{T}^\dagger$, $B^+ = \mathcal{T} b^+ \mathcal{T}^\dagger$.

The thermodynamic properties of a quark ensemble are known to be determined by solving the following problem. It is required to find such a statistical operator

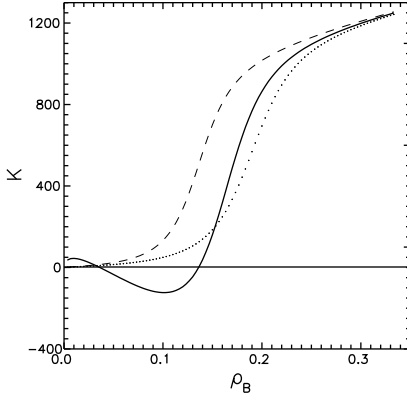
$$\xi = \frac{e^{-\beta \hat{H}_{\text{app}}}}{Z_0}, \quad Z_0 = \text{Tr} \{e^{-\beta \hat{H}_{\text{app}}}\}, \quad (3)$$

that at fixed mean charge

$$\bar{Q}_0 = \text{Tr}\{\xi Q_0\} = V \gamma \int d\tilde{\mathbf{p}} (n - \bar{n}), \quad (4)$$

$d\tilde{\mathbf{p}} = d\mathbf{p}/(2\pi)^3$, ($Q_0 = \bar{q}\gamma^0 q$), and fixed mean entropy

$$\begin{aligned} \bar{S} = & -\text{Tr}\{\xi S\} = \\ & - V \gamma \int d\tilde{\mathbf{p}} [n \ln n + (1 - n) \ln(1 - n) + \\ & + \bar{n} \ln \bar{n} + (1 - \bar{n}) \ln(1 - \bar{n})], \end{aligned} \quad (5)$$

FIG. 4: The compression module K in MeV.

($S = -\ln \xi$), provides a minimal value of mean energy of the quark ensemble

$$E = \text{Tr}\{\xi H\},$$

($H = \int d\mathbf{x} \mathcal{H}$). In other words, we are interested in the minimum of the following functional

$$\Omega = E - \mu \bar{Q}_0 - T \bar{S}, \quad (6)$$

where μ and T denote the Lagrangian multipliers for the chemical potential of the quark/baryon charge (which is usually taken to be three times larger than the baryon one in phenomenological considerations) and the temperature ($\beta = T^{-1}$), respectively. V is the volume the system is enclosed in, $\gamma = 2N_c$ (in the case of several quark flavors $\gamma = 2N_c N_f$, where N_f is the flavor number), $n = \text{Tr}\{\xi A^+ A\}$, $\bar{n} = \text{Tr}\{\xi B^+ B\}$ are the components of the corresponding density matrix.

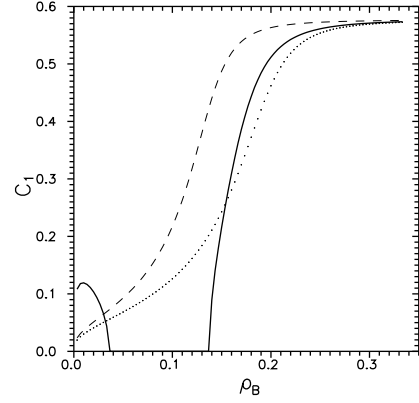
We restrict ourselves by considering the Bogolyubov–Hartree–Fock approximation in which the statistical operator is constructed on the basis of approximating effective Hamiltonian H_{app} , quadratic in creation and annihilation operators for quasiparticles acting in the corresponding Fock space with a vacuum state $|\sigma\rangle$. The average specific energy per quark $w = E/(V\gamma)$ results in [14]

$$w = \int d\tilde{\mathbf{p}} p_0 - \int d\tilde{\mathbf{p}} (1 - n - \bar{n}) p_0 \cos \theta - \frac{1}{2} \int d\tilde{\mathbf{p}} (1 - n - \bar{n}) \sin(\theta - \theta_m) M(\mathbf{p}), \quad (7)$$

where

$$M(\mathbf{p}) = 2G \int d\tilde{\mathbf{q}} (1 - n' - \bar{n}') \sin(\theta' - \theta'_m) F(\mathbf{p} + \mathbf{q}),$$

$\theta = 2\varphi$, $p_0 = (\mathbf{p}^2 + m^2)^{1/2}$, the primed variables, hereinafter correspond to the integration over momentum \mathbf{q} . The auxiliary angle θ_m is determined from the relation $\sin \theta_m = m/p_0$. The first term in Eq.(7) is introduced in view of normalizing in such a way to have the zero

FIG. 5: The first sound velocity C_1 .

energy of ground state when an interaction is switched off. This constant is unessential for the following consideration and may be omitted, however it should be kept in mind that it will appear as a regularizer in singular expressions further down the text.

The most stable extremals of the functional (7) are presented for comparison with the solid line for the NJL model and dashed one for the KKB model under normal conditions ($T = 0$, $\mu = 0$) in Fig.1. For the delta-like potential in coordinate space (the NJL model) the expression (7) diverges and to obtain the reasonable results the upper limit cutoff in the momentum integration Λ is introduced being one of the tuning model parameters along with the coupling constant G and current quark mass m . Below, we use one of the standard sets of the parameters for the NJL model [15]: $\Lambda = 631$ MeV, $G\Lambda^2/(2\pi^2) \approx 1.3$, $m = 5.5$ MeV, whereas the KKB model parameters are chosen in such a way that for the same quark current masses the dynamical quark ones in both NJL and KKB models coincide at vanishing quark momentum. The momentum p_ϑ (parameter) corresponds to the maximal attraction between quark and anti-quark. The value of this parameter inversed determines a characteristic size of quasiparticle. It is of order of $p_\vartheta \sim (mM_q)^{1/2}$, where M_q is a characteristic quark dynamical mass for the models considered, i.e. the quasiparticle size is comparable with the size of π -meson (Goldstone particle). It is a remarkable fact that the quasiparticle, as it is seen from Fig. 1, does not depend noticeably on the formfactor profile or, in other words, on the scale, but rather depends on the coupling constant. Using the properties of extremals the functional expression (7) can be transformed to the form (see [14])

$$w = \int d\tilde{\mathbf{p}} p_0 - \int d\tilde{\mathbf{p}} (1 - n - \bar{n}) P_0 + \frac{1}{4G} \int d\tilde{\mathbf{p}} d\tilde{\mathbf{q}} F(\mathbf{p} + \mathbf{q}) \tilde{M}(\mathbf{p}) \tilde{M}(\mathbf{q}), \quad (8)$$

where $P_0 = [\mathbf{p}^2 + M_q^2(\mathbf{p})]^{1/2}$ is the energy of quark quasi-

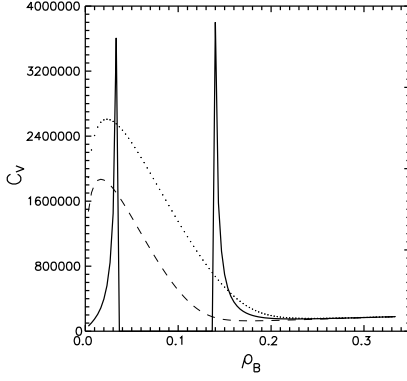


FIG. 6: The slope factor at low temperatures $\frac{1}{3}\pi^2 N_F$ in the thermal conductivity expression at constant volume $C_V = \frac{1}{3}\pi^2 N_F T$.

particle with the dynamical quark mass

$$M_q(\mathbf{p}) = m + M(\mathbf{p}) = m + \int d\mathbf{q} F(\mathbf{p} + \mathbf{q}) \widetilde{M}(\mathbf{q}) . \quad (9)$$

Below we omit often the arguments of corresponding functions for the mass and quasiparticle energy. Varying the functional (8) with respect to the density of induced quasiparticle mass \widetilde{M} (in such a form it is convenient to take variational derivatives[32]) we obtain the equation for dynamical quark mass as

$$M_q(\mathbf{p}) = m + 2G \int d\mathbf{q} (1 - n' - \bar{n}') \frac{M'_q}{P_0} F(\mathbf{p} + \mathbf{q}), \quad (10)$$

which corresponds exactly to the mean field approximation. In particular, under normal conditions ($T = 0$, $\mu = 0$) the dynamical quark mass in the NJL model is $M_q \sim 340$ MeV, whereas the dynamical quark mass of the KKB model is determined by the following equation

$$M(\mathbf{p}) = 2G \frac{M_q(\mathbf{p})}{P_0} . \quad (11)$$

In practice, it is convenient to use an inverse function $p(M_q)$. Then in the chiral limit $M_q = (4G^2 - \mathbf{p}^2)^{1/2}$, at $|\mathbf{p}| < 2G$, and $M_q = 0$ when $|\mathbf{p}| > 2G$. In this case the quark states with momenta $|\mathbf{p}| < 2G$ are degenerate in energy $P_0 = 2G$. Fig.2 demonstrates three branches of the equation (11) solutions for dynamical quark mass. The dots show the imaginary part of solutions which are generated at the point where two real solution branches are getting merged.

II. MEAN ENERGY AS A FUNCTIONAL OF QUANTUM LIQUID THEORY

The goal that we pursued while passing from the expression for specific energy (7) to Eq. (8) was to derive such a form that would easily be recognized as an energy functional of the Landau Fermi-liquid theory [16].

Some aspects of this theory are interesting and useful to be applied for comparing the results obtained in the NJL and KKB models. We will also discuss the first order phase transition which is apparently typical for interacting fermions (relativistic Fermi-liquid).

Thus, the second term in (8) describes the contributions coming from quark and antiquark quasiparticles with occupation numbers n and \bar{n} respectively. The unity in the expression $1 - n' - \bar{n}'$ corresponds to the vacuum fluctuations of quarks and antiquarks. The last term in (8) is due to the interaction of quasiparticles. The presence of contributions coming from antiparticles and the relativistic form of dynamics are those features which distinguish quark ensembles we study from the Fermi-liquids considered in condensed matter physics. The first variation of the functional (8) with respect to the particle (antiparticle) density leads (as it should be) to the energy of quasiparticle:

$$\frac{\delta w}{\delta n} = P_0 . \quad (12)$$

Consider, first, the situation of zero temperature and discuss some aspects of filling up the Fermi sphere by quarks. Let us assume that the momentum distribution of quarks (antiquarks) is determined by the following expressions taken at the $\beta \rightarrow 0$ limit

$$n = [e^{\beta(P_0 - \mu)} + 1]^{-1}, \quad \bar{n} = [e^{\beta(P_0 + \mu)} + 1]^{-1}, \quad (13)$$

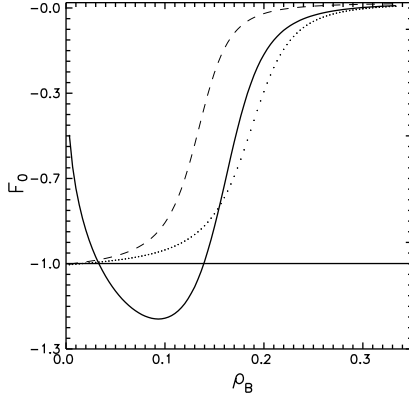
that is by the Fermi step function: $n = 1$, at $P_0 \leq \mu$ and $n = 0$ when $P_0 > \mu$. It is clear that for antiquarks $\bar{n} = 0$. The quark density is determined by using the Fermi momentum:

$$\rho = \frac{\gamma P_F^3}{6\pi^2}, \quad \rho = \frac{Q_0}{V}, \quad (14)$$

with the quark chemical potential that coincides with the quasiparticle energy on the Fermi surface, as it follows from the relation (12), i.e.

$$\mu = [P_F^2 + M_q^2(P_F)]^{1/2}. \quad (15)$$

The group velocity of quasiparticles on the Fermi surface $v_f = \partial P_0 / \partial \mathbf{p}|_{|\mathbf{p}|=P_F}$ is shown in Fig.3 as a function of baryon (quark) density (by definition, the baryon density is three times smaller than the quark one $\rho_B = \rho/3$). A solid line describes the NJL model, while a dashed one corresponds to the KKB model. There are points for comparison that show a version for the KKB model when the parameters are tuned in such a way that the π -meson masses coincide in the NJL and KKB models (similar notation is used below in Figs. 4–8). Tending the group velocity to unity in the region of normal nuclear densities corresponds to the chiral symmetry restoration when an induced quark mass tends to zero. The group velocity turns to zero for quarks with momenta $|\mathbf{p}| < 2G$ in the

FIG. 7: The factor F_0 of the Landau Fermi-liquid theory.

chiral limit in the KKB model. The negative group velocities in the NJL model correspond to the regions of instability (see below). The points in which the group velocity vanishes give rise to the peaks in the density of states on the Fermi surface N_F ,

$$N_F = \gamma \int d\tilde{\mathbf{p}} \delta(P_0 - \mu) = \frac{\gamma}{2\pi^2} P_F P_F^0 (1 + F_0)^{-1}, \quad (16)$$

$$F_0 = \frac{M_q}{P_F} \frac{dM_q}{dP_F},$$

where $P_F^0 = P_0|_{|\mathbf{p}|=P_F}$, $N_F = d\rho/d\mu$. For more detail on how to determine the parameter F_0 , see below. The interaction term in the functional (8) vanishes in an ideal gas and causes the derivative of quark dynamical mass in the Fermi momentum to turn to zero: $dM_q/dP_F = 0$. Let us define the density of states of an ideal gas as

$$\tilde{N}_F = \gamma/(2\pi^2) P_F P_F^0,$$

then the relation (16) can be written in the form:

$$N_F = \tilde{N}_F (1 + F_0)^{-1}.$$

Another important characteristic is a compression coefficient

$$K = 9\rho \frac{d\mu}{d\rho} = 3 \frac{P_F^2}{\mu} (1 + F_0). \quad (17)$$

Fig. 4 demonstrates the data for the NJL and KKB models. They are consistent with the specific values obtained for nuclear medium. One can also conclude that, in principle, these models admit a wide variety of equations of state including sufficiently restrictive ones. The negative values of the compression coefficient are not allowed and signal the region of instability. The first sound velocity which is determined by the relation

$$C_1^2 = \frac{K}{9\mu} = \frac{v_F^2}{3} (1 + F_0), \quad (18)$$

is shown in Fig. 5. When baryon densities are somewhat higher than the density of normal nuclear matter, the

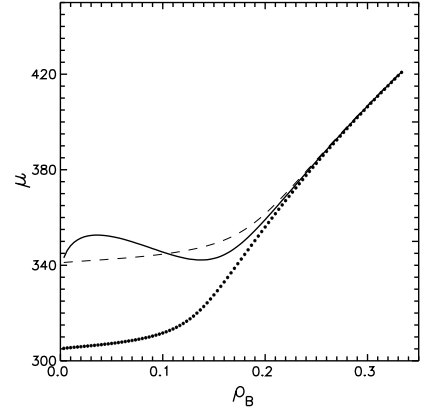


FIG. 8: Chemical potential in MeV.

sound velocity tends to its asymptotic value $C_1 = 1/\sqrt{3}$ which is a natural manifestation of the chiral symmetry restoration. If the sound velocity of an ideal Fermi-gas $\tilde{C}_1^2 = v_F^2/3$ is introduced in a way similar to the \tilde{N}_F definition, then the expressions (16), (18) can be endowed with the form whose physical meaning is an equality of flow coming through the Fermi sphere of quasiparticles of (imaginary) ideal Fermi-gas and interacting Fermi-liquid (that is, there basically is a relativistic analogue of the Luttinger theorem [17])

$$N_F C_1^2 = \tilde{N}_F \tilde{C}_1^2. \quad (19)$$

The thermal conductivity at a constant volume and a low temperature is given by the expression

$$C_V = \frac{1}{3} \pi^2 N_F T. \quad (20)$$

Fig. 6 shows the slope (the factor $\frac{1}{3}\pi^2 N_F$ in Eq.(20), $N_F = d\rho/d\mu$), as a function of baryon/quark density that demonstrates how informative it could be to measure the slope of a curve corresponding to the thermal conductivity. Yet another important characteristic of Fermi-liquid is defined by the second variational derivative, which for the functional (8) develops only a scalar component

$$f_0 = \frac{\delta^2 w}{\delta n^2} = \frac{M_q}{P_0} \frac{\delta M_q}{\delta n}. \quad (21)$$

For the Fermi-liquid at zero temperature, in particular, we have

$$f_0 = \frac{2\pi^2}{\gamma P_F P_F^0} \frac{M_q}{P_F} \frac{dM_q}{dP_F}.$$

For example, in the NJL model

$$\frac{M_q}{P_F} \frac{dM_q}{dP_F} = -\frac{P_F}{P_F^0} \frac{1}{I + \pi^2 m/(GM_q^3)},$$

$$I = \ln \frac{\Lambda + P_\Lambda^0}{P_F + P_F^0} - \frac{\Lambda}{P_\Lambda^0} + \frac{P_F}{P_F^0}.$$

where $P_\Lambda^0 = P_0|_{|\mathbf{p}|=\Lambda}$. In the KKB model

$$\frac{M_q}{P_F} \frac{dM_q}{dP_F} = -\frac{M M_q^2}{M_q^3 + m P_F^3}.$$

In particular, in the chiral limit (when $m = 0$) we have $(M_q/P_F)(dM_q/dP_F) = -1$. The collective oscillation modes of the Fermi-liquid, the so-called zero sound (the collisionless mode), are found by using the parameter

$$F_0 = \tilde{N}_F f_0 = \frac{M_q}{P_F} \frac{dM_q}{dP_F},$$

which is shown in Fig. 7. In particular, in the KKB model

$$F_0 = -\frac{M M_q^2}{M M_q^2 + (P_F^0)^2 m} \geq -1.$$

The zero sound oscillations are known to be determined by the solutions to the dispersion equation with a frequency parameter s (for details concerning this notation see the section devoted to the polarization operator) of the form:

$$F_0 = \frac{s}{2} \log \frac{s+1}{s-1} - 1. \quad (22)$$

When there is a repulsion in a system and the factor is positive $F_0 > 0$, the solutions to the dispersion equation $s = \lambda + i\eta$ describe continuous oscillations ($\eta = 0$). In the case of weak attraction, when $-1 < F_0 < 0$, the damped oscillations of zero sound are possible with a purely imaginary frequency ($\lambda = 0$) which is given by the solutions to the following equation:

$$F_0 + 1 = \eta \arctan(1/\eta).$$

When the strong attraction is available and $F_0 < -1$, the solutions reside on a second sheet of the complex plane s and describe the damped oscillations which are found from the solution to the equation

$$F_0 + 1 = \eta [-\pi + \arctan(1/\eta)].$$

It should, however, be recalled that these states of a Fermi-liquid are unstable (it will be discussed below). It is hardly possible to apply directly the consideration of zero sound given above to the situation of interacting quarks and antiquarks under studying, because here the contribution of vacuum fluctuations of antiquarks, which form along with quarks a chiral condensate, was completely ignored. On the other hand, zero sound oscillations are known to be interpreted as a bound state of a particle and hole in the vicinity of the Fermi sphere. Therefore, the excitations in a Fermi-liquid should be described (in our case) by taking into account an interference between the bound states of a quark and antiquark, as well as of a quark and a hole of the Fermi sphere (the

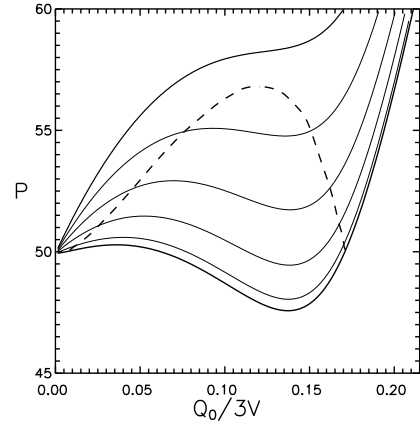


FIG. 9: The ensemble pressure P (MeV/fm³) is shown as a function of charge density Q_0 at temperatures $T = 0$ MeV, ..., $T = 50$ MeV with spacing $T = 10$ MeV. The lowest curve corresponds to zero temperature. The dashed curve shows the boundary of phase transition liquid-gas, see the text.

quantum numbers of that hole allows one to consider it as an antiparticle). We are doing that while calculating a respective polarization operator.

Turning now to the chemical potential of quasiparticles presented in Fig. 8 let us emphasize it is seen from the data for the NJL model that there is a region of occupied states almost degenerate with respect to the chemical potential with the vacuum chemical potential of a quasiparticle that quite naturally corresponds to the vanishing Fermi momentum. Similarly, the chemical potential of occupied states in the KKB model differs from that in vacuum by a small quantity proportional to the quark current mass

$$\frac{d\mu}{d\rho} = \frac{\mu}{\rho} \frac{v_F^2}{3} \left(1 + \frac{M_q}{P_F} \frac{dM_q}{dP_F} \right) \sim m. \quad (23)$$

All the states with momentum $|\mathbf{p}| < 2G$ are degenerate with respect to the chemical potential in the chiral limit. $M_q = (4G^2 - \mathbf{p}^2)^{1/2}$, $P_0 = 2G$, when $P_F < |\mathbf{p}| < 2G$, $M_q = 0$, $P_0 = |\mathbf{p}|$ if $|\mathbf{p}| < P_F$, and $|\mathbf{p}| > 2G$. Such a behavior of the chemical potential is a consequence of a rapid decrease of the dynamical quark mass with increasing Fermi momentum (see also (15)). It follows from Eq. (8) that the Fermi sphere is being filled as though from within. Those quarks with momenta smaller than the Fermi one $|\mathbf{p}| < P_F$ do not take part in forming a condensate. As a result, the quark dynamical mass can only decrease with the Fermi momentum increasing. This dynamical mass is independent of the quark momentum in the NJL model because of the approximation assumed. This dependence should be taken into account in more realistic case as an analysis of the KKB model shows.

It comes about that the pressure of some occupied states degenerate in the chemical potential almost coincides with that of vacuum (the pressure of a dilute Fermi-

gas) ($T = 0$)

$$P = -\frac{dE}{dV} = -\mathcal{E} + \mu \rho ,$$

where $\mathcal{E} = E/V$ is the specific energy. Below we analyze respective data in a more detail including the situation with nonzero temperature. The energy (and, hence, the pressure) of ensemble is a discontinuous functional of the quark current mass (see [11]) in the KKB model. The integrands in (8) are estimated then as follows

$$p_0 - P_0 + \frac{1}{4G} M^2 \sim -\frac{G m^2}{p^2} ,$$

and we find a linearly diverging integral for the specific energy of ensemble

$$w \sim -\int \frac{dp p^2}{2\pi^2} \frac{G m^2}{p^2} ,$$

despite the fact that the delta-like form factor in the momentum space is the strongest regularizer. It is paradoxical that any small value of the current mass m leads to the negative infinite energy of ensemble, while the expression $w|_{m=0}$ is well-defined in the chiral limit. Even more so, a similar divergence occurs in the case of a delta-like form factor in the coordinate space. This fact is concealed by introducing the cutoff momentum Λ in the NJL model. Now it looks quite sensible to consider the relative pressure of quark ensemble in comparison with a (formally infinite) vacuum value because of the singular character (mentioned above) of ensemble pressure in the KKB model. The pressure derivative in the ensemble density has the form: $dP/d\rho = \rho d\mu/d\rho$. Therefore, one can conclude by using an estimate given in (23) that the occupied states with momenta $|\mathbf{p}| < 2G$ are observed to degenerate with respect to the pressure ($\mathcal{E} = 2G\rho$, $\mu = 2G$) in the chiral limit in the KKB model. The deviations are proportional to the quark current mass beyond the chiral limit.

Now, we are able to analyse some thermodynamic properties of a system and to consider, first, the pressure of quark ensemble in detail

$$P = -\frac{dE}{dV} .$$

By definition, the volume derivative should be calculated at the constant mean entropy, $d\bar{S}/dV = 0$. Implimenting this constraint, one can, for example, extract the volume derivative of the chemical potential $d\mu/dV$. However, this approach cannot be implied because mean charge conservation might be broken. In fact, there is only one possibility to satisfy both conditions by introducing two independent chemical potentials for quarks and antiquarks separately. We use a symbol μ introduced earlier for the quark chemical potential, whereas the antiquark chemical potential is taken with an opposite charge and is denoted by $\bar{\mu}$. Then, we have

$$n = \frac{1}{e^{\beta(P_0 - \mu)} + 1} , \quad \bar{n} = \frac{1}{e^{\beta(P_0 + \bar{\mu})} + 1}$$

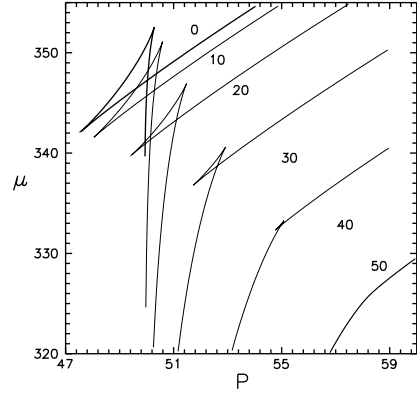


FIG. 10: The fragments of the isotherms shown in Fig. 9, see the text. The chemical potential μ (MeV) is plotted as a function of pressure P MeV/fm³. The top curve corresponds to the zero isotherm and following down with spacing 10 MeV till the isotherm 50 MeV (the lowest curve).

for the quark and antiquark densities, respectively. Some nonequilibrium states of quark ensemble could also be described on this way (formally with a loss of covariance, just similar to the electrodynamics as for the situation of electron–positron gas). However, we are here interested only in a special configuration when $\bar{\mu} = \mu$. The partial derivative of a specific energy dw/dV can be presented in the following form

$$\frac{dw}{dV} = \int d\tilde{\mathbf{p}} \left(\frac{dn}{d\mu} \frac{d\mu}{dV} + \frac{d\bar{n}}{d\bar{\mu}} \frac{d\bar{\mu}}{dV} \right) \left[p_0 \cos \theta - 2G \times \right. \\ \left. \times \sin \left(\theta - \theta_m \right) \int d\tilde{\mathbf{q}} \sin \left(\theta' - \theta'_m \right) \left(n' + \bar{n}' - 1 \right) F \right] .$$

Dealing with the definition of an induced quark mass (9) and presenting the trigonometric factors via the quark dynamical mass we find out the ensemble pressure as

$$P = -\frac{E}{V} - V 2N_c \int d\tilde{\mathbf{p}} \left(\frac{dn}{d\mu} \frac{d\mu}{dV} + \frac{d\bar{n}}{d\bar{\mu}} \frac{d\bar{\mu}}{dV} \right) P_0 . \quad (24)$$

The condition of mean charge conservation

$$\frac{d\bar{Q}_0}{dV} = \frac{\bar{Q}_0}{V} + V 2N_c \int d\tilde{\mathbf{p}} \left(\frac{dn}{d\mu} \frac{d\mu}{dV} - \frac{d\bar{n}}{d\bar{\mu}} \frac{d\bar{\mu}}{dV} \right) = 0 , \quad (25)$$

gives the first equation that interrelates the derivatives $d\mu/dV$ and $d\bar{\mu}/dV$. Here, a regularized expression for the mean charge of quarks and antiquarks is assumed modulo respective vacuum contribution.

Implimenting the condition of constant mean entropy $d\bar{S}/dV = 0$ in a similar way one can obtain the second equation of chemical potential derivatives system as follows

$$\int d\tilde{\mathbf{p}} \frac{dn}{d\mu} \ln \frac{n}{1-n} \frac{d\mu}{dV} - \int d\tilde{\mathbf{p}} \frac{d\bar{n}}{d\bar{\mu}} \ln \frac{\bar{n}}{1-\bar{n}} \frac{d\bar{\mu}}{dV} = \frac{\bar{S}}{2N_c V^2} . \quad (26)$$

Substituting the expressions $T \ln \frac{n}{1-n} = \mu - P_0$ and $T \ln \frac{\bar{n}}{1-\bar{n}} = -\bar{\mu} - P_0$ into this equation and collecting

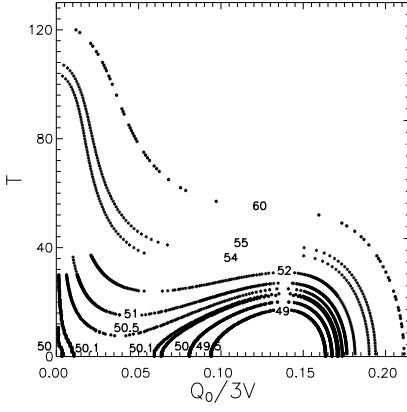


FIG. 11: Isobars of NJL model. Pressure in MeV/fm^3 is indicated next to each curve. Vacuum pressure corresponds to approximately $50 \text{ MeV}/\text{fm}^3$.

similar terms we come to the following equation

$$\int d\tilde{\mathbf{p}} \left(\frac{dn}{d\mu} \frac{d\mu}{dV} + \frac{d\bar{n}}{d\bar{\mu}} \frac{d\bar{\mu}}{dV} \right) P_0 = -\frac{\bar{S} T}{2N_c V^2} - \frac{\bar{Q}_0 \mu}{2N_c V^2}.$$

if the condition $\bar{\mu} = \mu$ and Eq. (25) are satisfied. Finally, we have for the pressure

$$P = -\frac{E}{V} + \frac{\bar{S} T}{V} + \frac{\bar{Q}_0 \mu}{V}. \quad (27)$$

Then the thermodynamic potential Ω should obey the following thermodynamic identity

$$\Omega = -PV = E - \mu \bar{Q}_0 - T \bar{S}, \quad (28)$$

as it should be. At low temperatures the antiquark contribution is small and thermodynamic description can be approximately developed by using the chemical potential μ only. If the antiquark contribution becomes significant, a thermodynamic description is more sophisticated and should obviously include the chemical potential $\bar{\mu}$ with additional condition $\bar{\mu} = \mu$. Fig. 9 shows the ensemble pressure P in MeV/fm^3 as a function of the charge density $Q_0/3V$ for various temperatures. The lowest curve is obtained at zero temperature. Next curves following upwards correspond to temperatures $T = 10 \text{ MeV}$, $T = 50 \text{ MeV}$ (an upper curve) with a step $T = 10 \text{ MeV}$. Let us also remember the pressure of vacuum for the NJL model was estimated in [11] to be 40 to $50 \text{ MeV}/\text{fm}^3$ which is quite consistent with that obtained in the bag model. It was also demonstrated that there is a region of instability within a certain interval of the Fermi momenta generated by the anomalous behavior of pressure $dP/dn < 0$ (see also [18]). Fig. 10 displays fragments of isotherms shown in Fig. 9 (but now in different coordinates) in the form of chemical potential as a function of the ensemble pressure. A top curve is obtained at zero temperature. The isotherms following below are shown in steps of 10 MeV . A lowest curve is obtained at temperature 50 MeV . It is clearly seen from the figure that there are states

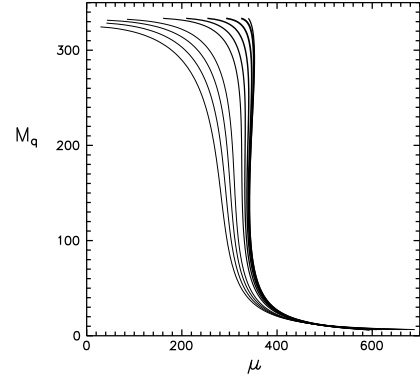


FIG. 12: The dynamical quark mass $|M_q|$ (MeV) as a function of chemical potential μ (MeV) at the temperatures $T = 0 \text{ MeV}$, \dots , $T = 100 \text{ MeV}$ with spacing $T = 10 \text{ MeV}$. The most right curve corresponds to zero temperature.

on the isotherms which are in thermodynamic equilibrium. The pressure and chemical potential are the same for these states (see the characteristic Van der Waals triangle with intersecting curves). The equilibrium points obtained are shown in Fig. 9 by a dashed curve. The points at which a dashed curve intersects with isotherm give a boundary for a gas—liquid phase transition. The respective line $P = \text{const}$ cuts off nonequilibrium and unstable fragments of isotherm and describes a mixed phase. The critical temperature turns out to be equal to $T_c \approx 46 \text{ MeV}$ with the critical charge density $\bar{Q}_0 \approx 0.12 \text{ charge}/\text{fm}^3$ for the above mentioned tuning parameters. Fig. 11 shows the isobars. The pressure next to each curve is given in MeV/fm^3 . The vacuum pressure corresponds to approximately $\sim 50 \text{ MeV}/\text{fm}^3$. It is possible to extrapolate isobars into the region of small charge densities, however, it is not really necessary. The figure clearly demonstrates the presence of dilute (a gas) and dense (a liquid) phases in the vicinity of the vacuum isobar.

Fig. 12 shows the quark dynamical mass M_q (in MeV) as a function of chemical potential μ (in MeV) for temperatures $T = 0 \text{ MeV}$, $T = 100 \text{ MeV}$ in steps of $T = 10 \text{ MeV}$. The rightmost curve corresponds to zero temperature. At low temperatures below 50 MeV the quark dynamical mass is a multivalued function of chemical potential. Fig. 13 shows the quark dynamical mass as a function of temperature at small charge density $Q_0 \sim 0$. This picture is easily recognizable in context of the NJL model. It is the latter that is implied in a scenario of chiral invariance restoration under extreme temperatures higher than 100 MeV and with a highly diluted quark ensemble. We have already noted (see also [11]) that the momentum p_θ , which corresponds to the strongest quark—antiquark attraction $d \sin \theta / dp = 0$, can be determined. For example, for the NJL model this parameter is equal to

$$p_\theta = (M_q m)^{1/2}. \quad (29)$$

Its inverse value is given by the characteristic effective size of a quasiparticle $r_\theta = p_\theta^{-1}$. From the behavior of

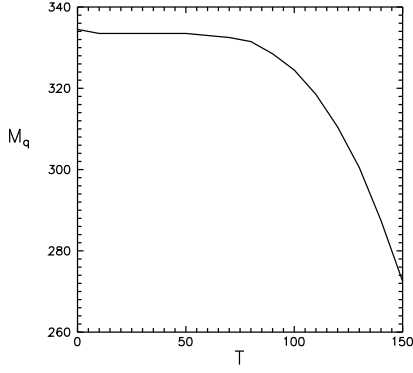


FIG. 13: The dynamical quark mass $|M_q|$ (MeV) as a function of temperature at the small value of charge density \mathcal{Q}_4 .

the quark dynamical mass as a function of temperature at small charge densities (see Fig. 13) one can conclude that a quasiparticle size grows with an energy increasing.

In [14] it was shown that if the quark chemical potential is defined as energy necessary to add (remove) one quasiparticle, $\mu = dE/dN$, then the chemical potential in vacuum coincides with the quark dynamical mass (see also (12), (15)). Therefore, it seems to be reasonable to consider a QCD phase diagram by starting from this value of the chemical potential, though formally it can be taken smaller than the quark dynamical mass. In particular, we exactly reproduce a standard picture [15], [19] by taking the chemical potential equal zero. The results obtained allows to conjecture that the phase transition of (partial) restoration of the chiral invariance could already be realized in nature as a mixed phase of physical vacuum and baryonic matter. An indirect confirmation of this hypothesis can be seen in degenerate excited states of some baryons (see, for instance, [20]). It is, however, clear that the data presented (in particular, on the temperature and density of a critical point position) should be understood as just an estimates. The critical temperature of a gas—liquid transition for nuclear matter extracted from experiment is estimated to be about 20 MeV. In addition, here (at $T = 0$) a gas component possesses the nonzero density of order of 0.01 of the normal nuclear density, whereas an observed value should correspond to physical vacuum, i.e., to zero baryon density. It should be noted that although such an uncertainty is inherent in the other predictions of chiral symmetry restoration phase transition which are widely discussed in many papers, they are somewhere around two to six normal nuclear matter densities.

III. POLARIZATION OPERATOR

Returning to the discussion of zero sound and excitations of a chiral condensate we would like also to remind that this knowledge is necessary for a more consistent

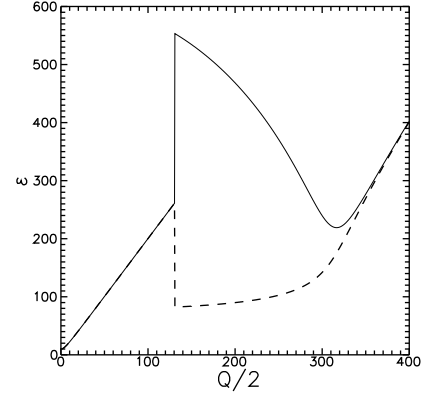


FIG. 14: Energies (in MeV) of π^- (dashed line) and σ^- (solid line) mesons as a function of momentum $Q/2$ (in MeV) ($T = 0$) for a gas of low baryon density such that $P_F \sim 130$ MeV.

analysis of the transition gas—liquid layer. To this end, we will need to know a polarization operator of the form

$$\Pi^\Gamma(p, q) = \int \frac{dk}{(2\pi)^4} i \pi^\Gamma(k + p, k - q), \quad (30)$$

where

$$\pi^\Gamma(k + p, k - q) = \text{Tr}\{S(k + p)\Gamma S(k - q)\Gamma\},$$

is a respective density of the polarization operator in the channels $\Gamma = 1, i\gamma_5, \gamma_\mu, \gamma_5\gamma_\mu$ with the Green function of quark with the dynamical mass M_q

$$S(k) = \frac{1}{\hat{k} + \hat{\mu} - M_q(\mathbf{k})}, \quad (31)$$

$\hat{\mu} = \mu\gamma^0$, where p, q are the incoming and outgoing external momenta of quark quasiparticles. It will be enough for our purposes to consider the quasiparticles with momenta $\mathbf{p} = \mathbf{q} = \mathbf{Q}/2$ in the center of mass frame. We analyse pseudoscalar and scalar channels, for which one can deduce

$$\begin{aligned} \Pi^{\pi, \sigma} &= N_c \int d\mathbf{k} F(\mathbf{k}) \left[\frac{a + b \varepsilon}{\varepsilon^2 - (E_{\mathbf{p}} + E_{\mathbf{q}})^2} + \frac{c}{\varepsilon - E_{\mathbf{p}} + E_{\mathbf{q}}} \right], \\ a &= (E_{\mathbf{p}} + E_{\mathbf{q}}) \left[2 - n_{\mathbf{p}} - n_{\mathbf{q}} \right] \left[\frac{Q^2/4 - \mathbf{k}^2 \mp M_{\mathbf{p}} M_{\mathbf{q}}}{E_{\mathbf{p}} E_{\mathbf{q}}} - 1 \right], \\ b &= [n_{\mathbf{q}} - n_{\mathbf{p}}] \left[\frac{Q^2/4 - \mathbf{k}^2 \mp M_{\mathbf{p}} M_{\mathbf{q}}}{E_{\mathbf{p}} E_{\mathbf{q}}} - 1 \right], \\ c &= [n_{\mathbf{p}} - n_{\mathbf{q}}] \left[\frac{Q^2/4 - \mathbf{k}^2 \mp M_{\mathbf{p}} M_{\mathbf{q}}}{E_{\mathbf{p}} E_{\mathbf{q}}} + 1 \right], \end{aligned} \quad (32)$$

where $\varepsilon = p_0 - q_0$ is the transferred energy, $M_{\mathbf{p}} = M_q(\mathbf{p})$, $E_{\mathbf{p}} = [\mathbf{p}^2 + M_q^2(\mathbf{p})]^{1/2}$, the quantity $F(\mathbf{k})$ is a form factor and for the kinematics chosen $\mathbf{p} = \mathbf{k} + \mathbf{Q}/2$ (then $n_{\mathbf{p}}$ is an occupation number for a quasiparticle with momentum

p). In particular, at zero temperature we have the Fermi step: $n_{\mathbf{p}} = n(E_{\mathbf{p}} - \mu)$. The similar notation is also used for a quasiparticle with momentum $\mathbf{q} = \mathbf{k} - \mathbf{Q}/2$.

The first term in Eq. (32) corresponds to the quark and anti-quark contributions, whereas the second one comes from the quark and hole configuration. It is easy to see that at $F(\mathbf{k}) = \delta(\mathbf{k})$ (in the KKB model) we have cubic dispersion relations to determine the bound states: $1 - 2G \Pi^{\pi,\sigma}(\varepsilon, \mathbf{Q}) = 0$. As an example, Fig. 14 shows the energies (in units of MeV) calculated of π -(dashed line) and σ -(solid line) mesons as functions of the momentum $Q/2$ (in units of MeV) at zero temperature for the gas with small baryon density corresponding to the Fermi momentum $P_F \sim 130$ MeV. The region of degeneracy, seen in Fig. 14 at low quark momenta, is a consequence of the above discussed fact that the Fermi sphere is filled from the inside, and quarks with momenta smaller than P_F do not participate in forming the quark dynamical mass. Such a behavior is not observed in the NJL model because of the approximation adopted (the quark mass is independent of the momentum). Fig. 15 shows the energies (in units of MeV) of π -(dashed line) and σ -(solid line) mesons as the functions of baryon density ($T = 0$). The dots indicate a branch corresponding to the quark-hole bound state which appears to be degenerate for π - and σ -mesons. Just these branches correspond to the third additional root of the dispersion equation mentioned above, albeit there are only two roots, (see discussion of the NJL model). To be specific, the quark momentum is assumed to be 50 MeV larger than the Fermi one but the hole momentum is 50 MeV smaller than the latter in this example. As it follows from Eq. (32), the polarization operator in the NJL model is defined by integrating over the running quark momentum k and is represented as a superposition of branches of the KKB model, which has already been mentioned in the introduction. The most significant contributions (for the kinematics we chose) are those coming from the terms denoted as a and c in Eq. (32). Integrating over the angle (it is more convenient to express the final formula by going to a nonsymmetric integration point, the corrections become negligibly small) one can obtain (at $T = 0$) the following results

$$\begin{aligned} \Pi^{\pi,\sigma} &= A^{\pi,\sigma} + B^{\pi,\sigma}, \\ A^{\pi,\sigma} &= \int_0^{\Lambda_{P_F}} \frac{dk k}{2\pi^2 Q} \left[\left(E_+ - E_- \right) \left(1 + \frac{E_+ + E_-}{2E_k} \right) - \right. \\ &\quad \left. - \frac{Q^2 - \varepsilon^2 + 2(M_q^2 \mp M_q^2)}{2E_k} \ln \left(\frac{\varepsilon + E_k + E_+}{\varepsilon + E_k + E_-} \frac{\varepsilon - E_k - E_+}{\varepsilon - E_k - E_-} \right) \right], \\ B^{\pi,\sigma} &= \int_0^{P_F} \frac{dk k}{2\pi^2 Q} \left[\left(E_+ - E_- \right) \left(1 - \frac{E_+ + E_-}{2E_k} \right) + \right. \\ &\quad \left. + \frac{Q^2 - \varepsilon^2 + 2(M_q^2 \mp M_q^2)}{2E_k} \ln \left(\frac{\varepsilon - E_k + E_+}{\varepsilon - E_k + E_-} \frac{\varepsilon + E_k - E_+}{\varepsilon + E_k - E_-} \right) \right], \end{aligned}$$

where $E_{\pm} = [(k \pm Q)^2 + M_q^2]^{1/2}$ and $E_k = [k^2 + M_q^2]^{1/2}$.

At small momentum Q the component B^{σ} is transformed into Eq. (22) with the parameter $s = E_F \varepsilon / (k_F Q)$. The first component $A^{\pi,\sigma}$ results from the contribution coming from a quark–antiquark pair, whereas the second one $B^{\pi,\sigma}$ arises due to the coupling of quark and hole residing in the vicinity of the Fermi sphere. It should be noted that for a quark ensemble we consider the medium properties which are mainly governed by the term $A^{\pi,\sigma}$ responsible for the quark–antiquark condensate, contrary to what we have in the condensed matter physics where the dominant contribution, as it is known, is given by $B^{\pi,\sigma}$. Therefore, the results obtained exclusively by using an analogy with the condensed matter physics should be taken with a grain of salt. In particular, in the present paper we have analysed in detail a situation with the zero sound description taken as an example illustrating just this point. The zero sound would represent in itself the highly damped oscillations described by the only scalar parameter F_0 while with no an antiquark presence. More accurate analysis shows that, for example, there is a stable branch of quark and hole excitations in the Fermi sphere in addition to a paired quark–antiquark state in the KKB model. We observe a regular mass convergence for π - and σ -mesons when baryon density increases by performing numerical integration in the NJL model. This effect is clearly related to the restoration of chiral symmetry. An influence of a bound quark–hole state in the Fermi sphere turns out to be insignificant. For instance, for the densities of order of normal nuclear matter the dispersion law changes by a few MeV when the quark and hole momentum differs more than 200 MeV, but there are no damped oscillations as it is in the KKB model.

One of the drawbacks of the models studied so far is the lack of quark confinement that is understood here simply as an impossibility to observe a single particle state with a regular (real) dispersion law. We see formally one quasiparticle can freely propagate, indeed. But adding just another quasiparticle can dramatically change the picture due to existence of a bound channel. For example, in the KKB model the bound states in scalar, pseudoscalar, vector, and axial-vector channels appear at any quasiparticles momenta (details can be found in [21]). In particular, the bound state energy, obtained by using the dispersion equation $1 - 2G \Pi = 0$, has the form

$$\varepsilon_{\pi,\sigma}^2 = \left(E_{\mathbf{p}} + E_{\mathbf{q}} \right)^2 - 2G \frac{E_{\mathbf{p}} + E_{\mathbf{q}}}{E_{\mathbf{p}} E_{\mathbf{q}}} \left(E_{\mathbf{p}} E_{\mathbf{q}} \pm M_{\mathbf{p}} M_{\mathbf{q}} - \mathbf{p} \mathbf{q} \right),$$

in π and σ channels (an upper sign corresponds to the pseudoscalar channel). The first term in this expression is the energy of free particle motion. The second one is strictly positive at any momenta p and q and plays a role of binding energy in π and σ channels (only in the configuration of $q = p$ the binding energy vanishes for a scalar channel). Similarly, one can show that a quark and antiquark are always coupled in vector and axial–vector channels, i.e. the scattering matrix is always singular excepting a tensor channel where it is trivial because of the

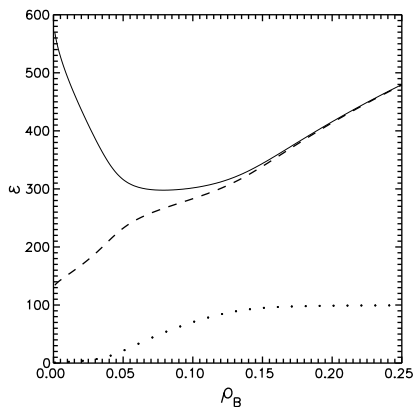


FIG. 15: Energies (in MeV) of π^- (dashed line) and σ^- (solid line) mesons as a function of baryon density ($T = 0$). The branch corresponding to a bound quark-hole state is shown by dots $Q_q = -Q_h = 50$ MeV.

initial interaction Hamiltonian that is taken as a product of two color currents. Similar bound states exist in a diquark channel. As a consequence, the states with any number of quark quasiparticles turn out to be the bound states in the channels we have just mentioned. The same behavior is observed in the NJL model where the bound states appear for the quarks with momenta somewhat lower than the cutoff momentum, i.e. the scattering matrix is also singular within this momentum interval as in the KKB model. It seems the bound states appear rather due to the fermion correlations than a physical influence of field that is familiar in the quantum electrodynamics. Then, in order to understand what may take place beyond the cutoff momentum one has apparently to study the appropriate nonlocal models.

IV. TRANSITION LAYER BETWEEN GAS AND LIQUID

The concept of a mixed phase of physical vacuum and baryonic matter would receive the substantial confirmation if we are able to demonstrate an existence of the boundary (transition) layer where a transformation of the quark ensemble from one aggregate state to another takes place. As it was argued above the indicative characteristic to explore a homogeneous phase (at finite temperature) is the mean charge (density) of ensemble. All the other characteristics, for example, a chiral condensate, dynamical quark mass, etc. can be reconstructed if one knows the ensemble mean charge. So, here we analyse a specific case of the surface (transition) layer at zero temperature.

We assume that the quark ensemble parameters in a gaseous phase are approximately the same as those at zero charge $\rho_g = 0$, i.e. as in vacuum (minor differences in pressure, chemical potential and quark condensate are neglected). The dynamical quark mass develops here the

maximal value, and it is $M = 335$ MeV for the parameter choice standard for the NJL model. Then as the Van der Waals diagram shows a liquid phase, being in equilibrium with a gas phase, gains the density $\rho_l = 3 \times 0.185$ charge/fm³ (by some reason which becomes clear below we correct it to take the value $\rho_l = 3 \times 0.157$ charge/fm³). The detached factor 3 here links again the magnitudes of quark and baryon matter densities. The quark mass is approximately $M^* \approx 70$ MeV in this phase. Hereafter we focus on describing two adjoining semi-infinite layers (i.e. assuming a plane symmetry of the corresponding one-dimensional problem).

The precursor experience teaches that an adequate description of heterogeneous states can be reached with the mean field approximation [22]. In our particular case it means making use the corresponding effective quark-meson Lagrangian [23] (functional of the Ginzburg-Landau type)

$$\mathcal{L} = -\bar{q} (\hat{\partial} + M) q - \frac{1}{2} (\partial_\mu \sigma)^2 - U(\sigma) - \frac{1}{4} F_{\mu\nu} F_{\mu\nu} - \frac{m_v^2}{2} V_\mu V_\mu - g_\sigma \bar{q} q \sigma + i g_v \bar{q} \gamma_\mu q V_\mu, \quad (33)$$

where

$$F_{\mu\nu} = \partial_\mu V_\nu - \partial_\nu V_\mu, \quad U(\sigma) = \frac{m_\sigma^2}{2} \sigma^2 + \frac{b}{3} \sigma^3 + \frac{c}{4} \sigma^4,$$

and σ is the scalar field, V_μ is the field of vector mesons, m_σ , m_v are the masses of scalar and vector mesons and g_σ , g_v are the coupling constants of quark-meson interaction. The $U(\sigma)$ potential includes the nonlinear σ field interaction terms up to the fourth order, for example. For the sake of simplicity we do not include the contributions coming from the pseudoscalar and axial-vector mesons.

The meson component of such a Lagrangian should be self-consistently treated by considering the corresponding quark loops. Here we do not see any reason to go beyond the well elaborated and reliable one loop approximation (33) [23], although recently the considerable progress has been reached in scrutinizing the non-homogeneous quark condensates by applying the powerful methods of exact integration [24]. Here we believe it is more practical to adjust phenomenologically the effective Lagrangian parameters basing on the transparent physical picture. It is easy to see that handling (33) one loop approximation we come, in actual fact, to the Walecka model [25] but adopted for the quarks. In what follows we are working with the designations of that model and do hope it does not lead to the misunderstandings.

In the context of our paper we propose to interpret Eq. (33) in the following way. Each phase might be considered, in a sense, with regard to another phase as an excited state which requires the additional (apart from a charge density) set of parameters (for example, the meson fields) for its complete description, and those are characterizing the measure of deviation from the equilibrium state. Then the crucial question becomes whether it is

possible to adjust the parameters of effective Lagrangian (33) to obtain the solutions in which the quark field interpolates between the quasiparticles in the gas (vacuum) phase and the quasiparticles of the filled-up states. For all that the density of the filled-up state ensemble should asymptotically approach the equilibrium value of ρ_l and should turn to the zero value in the gas phase (vacuum).

The scale inherent in this problem may be assigned with one of the mass referred in the Lagrangian (33). In particular, we bear in mind the dynamical quark mass in the vacuum M . Besides, there are another four independent parameters in the problem and in order to compare them with the results of studying a nuclear matter we employ the form characteristic for the (nuclear) Walecka model

$$C_s = g_\sigma \frac{M}{m_\sigma}, \quad C_v = g_v \frac{M}{m_v}, \quad \bar{b} = \frac{b}{g_\sigma^3 M}, \quad \bar{c} = \frac{c}{g_\sigma^4}.$$

Parameterizing the potential $U(\sigma)$ as $b_\sigma = 1.5 m_\sigma^2 (g_\sigma/M)$, $c_\sigma = 0.5 m_\sigma^2 (g_\sigma/M)^2$ we come to the sigma model whereas the choice $b = 0$, $c = 0$ results in the Walecka model. As to standard nuclear matter application the parameters b and c demonstrate vital model dependent character and are quite different from the parameter values of sigma model. Truly, in that case their values are also regulated by additional requirement of an accurate description of the saturation property. On the other hand, for the quark Lagrangian (33) we could intuitively anticipate some resemblance with the sigma model and, hence, could introduce two dimensionless parameters η and ζ in the form of $b = \eta b_\sigma$, $c = \zeta^2 c_\sigma$ which characterize some fluctuations of the effective potential. Then the scalar field potential is presented as follows

$$U(\sigma) = \frac{m_\sigma^2}{8} \frac{g_\sigma^2}{M^2} \left(4 \frac{M^2}{g_\sigma^2} + 4 \frac{M}{g_\sigma} \eta \sigma + \zeta^2 \sigma^2 \right) \sigma^2.$$

The meson and quark fields are determined by solving the following system of the stationary equations

$$\begin{aligned} \Delta \sigma - m_\sigma^2 \sigma &= b \sigma^2 + c \sigma^3 + g_\sigma \rho_s, \\ \Delta V - m_v^2 V &= -g_v \rho, \\ (\hat{\nabla} + M^*) q &= (E - g_v V) q, \end{aligned} \quad (34)$$

where $M^* = M + g_\sigma \sigma$ is the running value of dynamical quark mass, E stands for the quark energy and $V = -iV_4$. The density matrix describing the quark ensemble at $T = 0$ has the form

$$\xi(x) = \int_{P_F} d\tilde{\mathbf{p}} q_{\mathbf{p}}(x) \bar{q}_{\mathbf{p}}(x),$$

in which \mathbf{p} is the quasiparticle momentum and the Fermi momentum P_F is defined by the corresponding chemical potential. The densities ρ_s and ρ at the right hand sides of Eq. (34) are by definition

$$\rho_s(x) = \text{Tr} \{ \xi(x), 1 \}, \quad \rho(x) = \text{Tr} \{ \xi(x), \gamma_4 \}.$$

Here we confine ourselves to the Thomas–Fermi approximation while describing the quark ensemble. Then the densities which we are interested in are given with some local Fermi momentum $P_F(x)$ as

$$\begin{aligned} \rho &= \gamma \int_{P_F} d\tilde{\mathbf{p}} = \frac{\gamma}{6\pi^2} P_F^3, \\ \rho_s &= \gamma \int_{P_F} d\tilde{\mathbf{p}} \frac{M^*}{E} = \\ &= \frac{\gamma}{4\pi^2} M^* P_F^2 \left\{ \left(1 + \lambda^2 \right)^{1/2} - \frac{\lambda^2}{2} \ln \left[\frac{(1 + \lambda^2)^{1/2} + 1}{(1 + \lambda^2)^{1/2} - 1} \right] \right\}, \end{aligned} \quad (35)$$

where γ is a quark gamma-factor which for one flavour is $\gamma = 2N_c$, $E = (\mathbf{p}^2 + M^{*2})^{1/2}$ and $\lambda = M^*/P_F$. Under assumption adapted the ensemble chemical potential is constant and, therefore, a local value of the Fermi momentum is defined by the running value of dynamical quark mass and vector field as

$$\mu = M = g_v V + \left(P_F^2 + M^{*2} \right)^{1/2}. \quad (36)$$

Now we should tune the Lagrangian parameters in Eq. (33). For asymptotically large distances (in a homogeneous phase) we may neglect the gradients of scalar and vector fields and the equation for scalar field of the system (34) leads to the first equation that relates the parameters C_s , C_v , \bar{b} , \bar{c} as

$$\frac{M^2(M^* - M)}{C_s^2} + \bar{b} M(M^* - M)^2 + \bar{c}(M^* - M)^3 = -\rho_s. \quad (37)$$

The vector field asymptotically is given by the ensemble density $V = C_v^2 \rho / (g_v M^2)$. The second equation derived from the relation (36) for the chemical potential looks like

$$M = \frac{C_v^2 \rho}{M^2} + \left(P_F^2 + M^{*2} \right)^{1/2}. \quad (38)$$

If we know the liquid density we obtain the Fermi momentum ($P_F = 346$ MeV) from (35) and applying the identities (37), (38) we have for the particular case $b = 0$, $c = 0$ that $C_s^2 = 25.3$, $C_v^2 = -0.471$, i.e. the vector component C_v^2 is small (compared to C_s^2) and acquires a negative value that is unacceptable. Apparently, it looks necessary to abandon the contribution coming from the vector field or to reduce the dynamical quark mass M^* up to the value which retains the identity (38) valid with positive C_v^2 or even zero value. In the gaseous phase the dynamical quark mass can also be corrected to the value larger than the vacuum value. It is clear that in the situation of the liquid with the density $\rho_l = 3 \times 0.185 \text{ ch/fm}^3$ the dynamical quark mass should coincide (or exceed) $M = 346$ MeV in the gaseous phase. However, here we

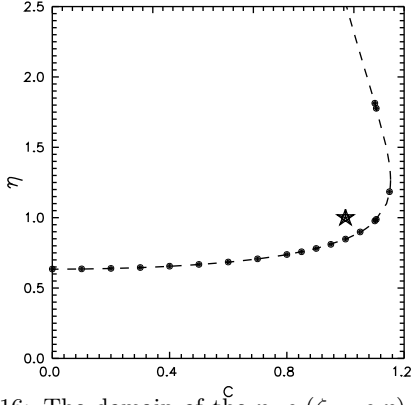


FIG. 16: The domain of the η, c ($\zeta = c \eta$)-plot in which an increase of specific energy occurs, see the text. The dots represent a stable kink. The star shows the position of canonical (chiral) kink, see the text.

correct the liquid density (as it was argued above) to decrease its value up to $\rho_l = 3 \times 0.157 \text{ ch/fm}^3$ which is quite acceptable in the nucleation capacity. In fact, this possibility can be simply justified by another choice of the NJL model parameters. Thus, we obtain at $\bar{M} = 70 \text{ MeV}$ and $b = 0, c = 0$ that $C_s^2 = 28.4, C_v^2 = 0.015$, i.e. we have a small but positive value for the vector field coefficient. At the same time, being targeted here to estimate the surface tension effects only we do not strive for the precise fit of parameters. In the Walecka model these coefficients are $C_s^2 = 266.9, C_v^2 = 145.7, (b = 0, c = 0)$. Moreover, there is another parameter set with $C_s^2 = 64., C_v^2 \approx 0$ [26] but it is rooted in an essential nonlinearity of the sigma-field due to the nontrivial values of the coefficients b and c . The option (formally unstable) with negative c (b) has been also discussed.

The coupling constant of scalar field is fixed by the standard (for the NJL model) relation between the quark mass and the π -meson decay constant $g_\sigma = M/f_\pi$ (we put $f_\pi = 100 \text{ MeV}$) although there is no any objection to treat this coupling constant as an independent parameter. As a result of all agreements done we have for the σ -meson mass $m_\sigma = g_\sigma M/C_s$. In principle, we could even fix the σ -meson mass and coupling constant g_σ but all relations above mentioned lead eventually to quite suitable values of the σ -meson mass as will be demonstrated below. The vector field plays, as we see, a secondary role because of the small magnitude of constant C_v . Then taking the vector meson mass as $m_v \approx 740 \text{ MeV}$ (slightly smaller value than the mass of ω -meson because of simple technical reason only) we calculate the coupling constant of vector field from the relation similar to the scalar field $m_v = g_v M/C_v$. Amazingly, its value comes about steadily small being compared to the value characteristic for the NJL model $g_v = \sqrt{6}g_\sigma$. However, at the values of constant C_v which we are interested in it is very difficult to maintain the reasonable balance and to be specific in this paper we prefer to choose the massive

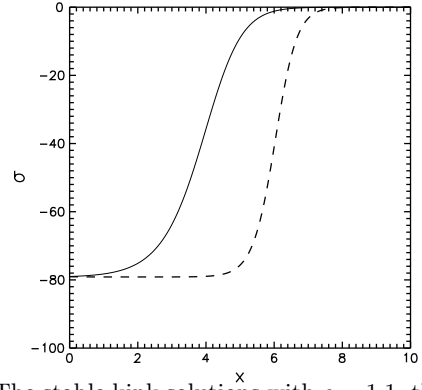


FIG. 17: The stable kink solutions with $c = 1.1$, the solid line corresponds to $\eta \approx 0.977$ ($m_\sigma \approx 468 \text{ MeV}$) and the dashed line corresponds to $\eta \approx 1.813$ ($m_\sigma \approx 690 \text{ MeV}$), x is given in the units of fm and σ is given in MeV .

vector field. Actually, it is unessential because we need this parameter (as we remember) to estimate the vector field strength only.

The key point of our interest here is the surface tension coefficient [26] which can be defined as

$$u_s = 4\pi r_o^2 \int_{-\infty}^{\infty} dx \left[\mathcal{E}(x) - \frac{\mathcal{E}_l}{\rho_l} \rho(x) \right]. \quad (39)$$

The parameter r_o will be discussed in the next section at considering the features of quark liquid droplet, and for the present we would like to notice only that for the parameters considered its magnitude for $N_f = 1$ is around $r_o = 0.79 \text{ fm}$. Recalling the factor $3^{1/3}$ which connects the baryon and quark numbers, we find the magnitude ($\tilde{r}_o = 3^{1/3} 0.79 \approx 1.14 \text{ fm}$) in full agreement with the magnitude standard for the nuclear matter calculations (in the Walecka model) $\tilde{r}_o = 1.1\text{--}1.3 \text{ fm}$.

In order to proceed we calculate $\mathcal{E}(x)$ in the Thomas-Fermi approximation as

$$\begin{aligned} \mathcal{E}(x) = & \gamma \int^{P_F(x)} \Phi [\mathbf{p}^2 + \bar{M}^*(x)]^{1/2} + \\ & + \frac{1}{2} g_v \rho(x) V(x) - \frac{1}{2} g_\sigma \rho_s(x) \sigma(x). \end{aligned}$$

And to give some idea for the 'setup' prepared we present here the characteristic parameter values for some fixed b and c with $\rho_l = 3 \times 0.157 \text{ ch/fm}^3$. In the liquid phase they are $\bar{M} = 70 \text{ MeV}$ ($P_F = 327 \text{ MeV}$) and $e_l = 310.5 \text{ MeV}$ (index l stands for a liquid phase and $e(x) = \mathcal{E}(x)/\rho(x)$ defines the density of specific energy). Both relations (37) and (38) are obeyed by this state. There exist the solution with larger value of quark mass $\bar{M} = 306 \text{ MeV}$, ($P_F = 135 \text{ MeV}$) (we have faced the similar situation in the first section dealing with the gas of quark quasiparticles) and $e = 338 \text{ MeV} \sim e_g$ (e_g is the specific energy in the gas phase) that satisfies both equations as well. The

specific energy of this solution occurs to be larger than specific energy of the previous solution. It is also worthwhile to mention the existence of intermediate state corresponding to the saturation point with the mass $M^* = 95$ MeV, ($P_F = 291$ MeV) and $e = 306$ MeV. Obviously, it is the most favorable state with the smallest value of specific energy (and with the zero pressure of quark ensemble), and the system can fall into this state only in the presence of significant vector field. This state (already discussed in the first section) corresponds to the minimal value of chemical potential ($T = 0$) and can be reached at the densities typical for the normal nuclear matter. However, Eq. (38) is not valid for this state.

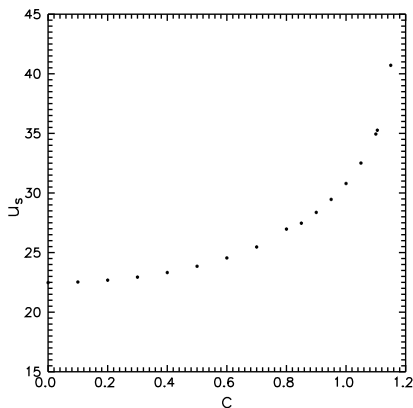


FIG. 18: The surface tension coefficient u_s in MeV as a function of parameter c ($\zeta = c \eta$) for the curve of stable kinks (with $\eta \leq 1.2$).

Two another parameters η , ζ are fixed by looking through all the configurations in which the solution of equation system (34) with stable kink of the scalar field does exist and describes the transition of quarks from the gaseous phase to the liquid one. First, it is reasonable to scan the η , c ($\zeta = c \eta$)-plane, in order to identify the domain in which the increase of specific energy $\mathcal{E} - \mathcal{E}_l \rho/\rho_l \leq 0$ is revealed at running through all possible states which provide the necessary transition (without taking into account the field gradients). In practice one need to follow a simple heuristic rule. The state with $P_F \sim 1$ MeV (i.e. e and the corresponding ρ) and the state of characteristic liquid energy \mathcal{E}_l (together with ρ_l) should be compared while scanning the Lagrangian parameters η and c . Just the domain in which they are commensurable could provide us with the solutions which we are interested in and Fig. 5 shows its boundary. The curve could be continued beyond the value $\eta = 2.5$ but the values of corresponding parameter η are unrealistic and not shown in the plot.

We calculate the solution of equation system (34) numerically by the Runge-Kutta method with the initial conditions $\sigma(L) \approx 0$, $\sigma'(L) \approx 0$ imposed at the large distance $L \gg t$, where t is a characteristic thickness of transition layer (about 2 fm). Such a simple algorithm

occurs quite suitable if the vector field contribution is considered as a small correction (what just takes place in the situation under consideration) and is presented as

$$V(x) = \frac{1}{2m_v} \int_{-L}^L dz e^{-m_v|x-z|} g_v \rho(z),$$

where the charge (density) ρ is directly defined by the scalar field. We considered the solutions including the contribution of the vector field as well and the corresponding results confirm the estimates obtained.

Rather simple analysis shows the interesting solutions are located along the boundary of discussed domain. Some of those are depicted in Fig. 16 as the dots. Fig. 17 shows the stable kinks of σ -field with the parameter $c = 1.1$ for two existing solutions with $\eta \approx 0.977$ ($m_\sigma \approx 468$ MeV) (solid line) and $\eta \approx 1.813$ ($m_\sigma \approx 690$ MeV) (dashed line). For the sake of clarity we consider the gas (vacuum) phase is on the right. Then the asymptotic value of σ -field on the left hand side ($\sigma \approx 80$ MeV) corresponds to $M^* = 70$ MeV. The thickness of transition layer for the solution with $\eta \approx 0.977$ is $t \approx 2$ fm whereas for the second solution $t \approx 1$ fm.

Characterizing the whole spectrum of the solutions obtained we should mention that there exist another more rigid (chiral) kinks which correspond to the transition into the state with the dynamical quark mass changing its sign, i.e. $M \rightarrow -M$. In particular, the kink with the canonical parameter values $\eta = 1$, $c = 1$ is clearly seen (marked by the star in Fig. 16) and its surface tension coefficient is about $2m_\pi$ (m_π is the π -meson mass). The most populated class of solutions consists of those having the meta-stable character. The system comes back to the starting point (after an evolution) pretty rapidly, and usually the σ -field does not evolve in such an extent to reach the asymptotic value (which corresponds to the dynamical quark mass in the liquid phase $M^* = 70$ MeV). Switching on the vector field changes the solutions insignificantly (for our situation with small C_v it does not exceed 2 MeV in the maximum).

The surface tension coefficient u_s in MeV for the curve of stable kinks with parameter $\eta \leq 1.2$ as the function of parameter c ($\zeta = c \eta$) is depicted in Fig. 18. The σ -meson mass at $c \approx 0$ is $m_\sigma \approx 420$ MeV and changes smoothly up to the value $m_\sigma \approx 500$ MeV at $c \approx 1.16$ (the maximal value of the coefficient c beyond which the stable kink solutions are not observed). In particular, $m_\sigma \approx 450$ MeV at $c = 1$. Two kink solutions with $c = 1.1$ for $\eta \approx 0.977$ and for $\eta \approx 1.813$ (shown in Fig. 17, and the second one is not shown in Fig. 18) have the tension coefficient values $u_s \approx 35$ MeV and $u_s \approx 65$ MeV, correspondingly. The maximal value of tension coefficient for the normal nuclear matter does not exceed $u_s = 50$ MeV. The nuclear Walecka model claims the value $u_s \approx 19$ MeV [26] as acceptable and calculable. The reason to have this higher value of surface tension coefficient for quarks is rooted in the different values of

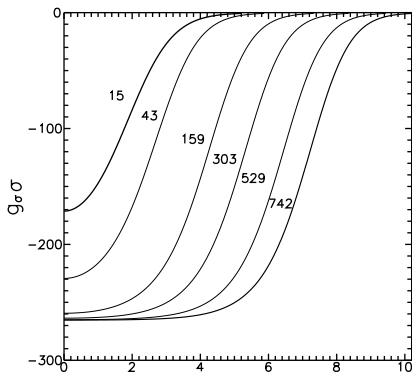


FIG. 19: σ -field (MeV) as a function of the distance r (fm) for several solutions of the equation system (34) which are characterized by the net quark number N_q written down to the left of each curve.

the mass deficit. Indeed, for nuclear matter it does not exceed $M^* \approx 0.5M$ albeit more realistic values are considered around $M^* \approx 0.7M$ and for the quark ensemble the mass deficit amounts to $M^* \approx 0.3M$. We are also able to estimate the compression coefficient of quark matter K which occurs significantly larger than the nuclear one. Actually, we see quite smooth analogy between the results obtained and the results of bag soliton model [27]. The thermodynamic treatment developed in the present paper allows us to formulate the adequate boundary conditions for the bag in physical vacuum and to diminish considerably the uncertainties in searching the true soliton Lagrangian. We believe, it was also shown here, that to single out one soliton solution among others (including even those obtained by the exact integration method [24]), which describes the transitional layer between two media, is not easy problem if the boundary conditions above formulated are not properly imposed.

V. DROPLET OF QUARK LIQUID

The results of previous sections have led us to put the challenging question about the creation and properties of finite quark systems or the droplets of quark liquid which are in equilibrium with the vacuum state. Thus, as a droplet we imply the spherically symmetric solution of the equation system (34) for $\sigma(r)$ and $V(r)$ with the obvious boundary conditions $\sigma'(0) = 0$ and $V'(0) = 0$ in the origin (the primed variables denote the first derivatives in r) and rapidly decreasing at the large distances $\sigma \rightarrow 0$, $V \rightarrow 0$, when $r \rightarrow \infty$.

A quantitative analysis of similar nuclear physics models which includes the detailed tuning of parameters is usually based on the comprehensive fitting of available experimental data. This way is obviously irrelevant in studying the quark liquid droplets. This global difficulty dictates a specific tactics of analyzing. We propose to

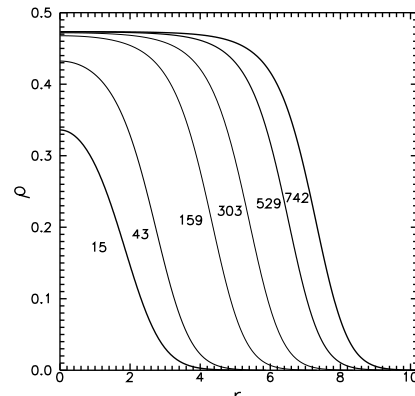


FIG. 20: Distribution of the quark density ρ (ch/fm³) for the corresponding solutions presented in Fig. 20.

start, first of all, with selecting the parameters which could be worthwhile to play a role of physical observables. Naturally, the total baryon number which phenomenologically (via factor 3) related to the number of valence quark in an ensemble is a reasonable candidate for this role. Besides, the density of quark ensemble $\rho(r)$, the mean size of droplet R_0 and the thickness of surface layer t look like suitable for such an analysis.

It is argued above that the vector field contribution is negligible because of the small value of coefficient C_v compared to the C_s magnitude, and we follow this conclusion (or assumption) albeit understand it is scarcely justified in the context of finite quark system. Thus, we put down $g_v = 0$, $V = 0$ in what follows and it simplifies all the calculations enormously.

Fig. 19 shows the number of solutions (σ -field in MeV) to the system (34) at $N_f = 1$ and Fig. 20 presents the corresponding distributions of ensemble density ρ (ch/fm³). The parameters C_s , C_v , b and c are derived by the same algorithm as in the previous section, i.e. the chemical potential of quark ensemble $M = 335$ MeV (and $\sigma \rightarrow 0$) is fixed at the spatial infinity. The filled-up states (of a liquid) are characterized by the parameters $M^* = 70$ MeV, $\rho_0 = \rho_l = 3 \times 0.157$ ch/fm³. The σ -meson mass and the coupling constant g_σ are derived at fixed coefficients η and ζ , and they just define the behaviour of solutions $\sigma(r)$, $\rho(r)$, etc. The magnitudes of functions $\sigma(r)$ and $\rho(r)$ at origin are not strongly correlated with the values characteristic for the filled-up states and are practically determined by solving the boundary value problem for system (34). In particular, the solutions presented in Fig. 19 have been received with the running coefficient η at $\zeta = \eta$. The most relevant parameter (instead of η) from the physical view point is the total number of quarks in the droplet N_q (as discussed above) and it is depicted to the left of each curve. (The variation of M^* and f_π could be considered as well instead of two mentioned parameters η and ζ .)

Analyzing the full spectrum of solutions obtained by scanning one can reveal a recurrent picture (at a certain

TABLE I: Results of fitting by the Fermi distribution with $N_f = 1$, $\tilde{\rho}_0$ (ch/fm³), R_0 , t , r_0 (fm), b (fm⁻¹), m_σ (MeV).

N_q	$\tilde{\rho}_0$	R_0	b	t	r_0	m_σ	η
15	0.34	1.84	0.51	2.24	0.74	351	0.65
43	0.43	2.19	0.52	2.28	0.75	384	0.73
159	0.46	4.19	0.52	2.29	0.77	409	0.78
303	0.47	5.23	0.52	2.29	0.78	417	0.795
529	0.47	6.37	0.52	2.27	0.79	423	0.805
742	0.47	7.15	0.52	2.27	0.79	426	0.81

scale) of kink-droplets which are easily parameterized by the total number of quarks N_q in a droplet and by the density ρ_0 . These characteristics are obviously fixed at completing the calculations. The sign which allows us to single out these solutions is related to the value of droplet specific energy (see below).

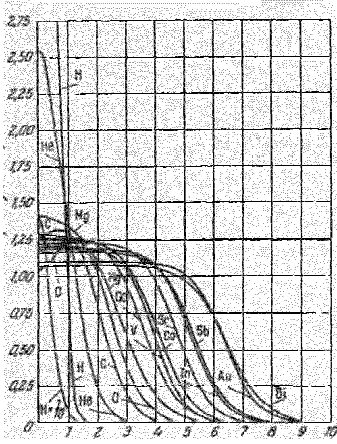


FIG. 21: Measured nuclear charge distributions (Hofstadter).

Table I exhibits the results of fitting the density $\rho(r)$ with the Fermi distribution

$$\rho_F(r) = \frac{\tilde{\rho}_0}{1 + e^{(R_0 - r)/b}}, \quad (40)$$

where $\tilde{\rho}_0$ is the density in origin, R_0 is the mean size of droplet and the parameter b defines the thickness of surface layer $t = 4 \ln(3)b$. Besides, the coefficient r_0 which is absorbed in the surface tension coefficient (39), the σ -meson mass, $R_0 = r_0 N_q^{1/3}$ and the coefficient η at which all other values have been obtained are also presented in the Table I.

The curves plotted in the Fig. 19 and results of Table I justify to conclude that the density distributions at $N_q \geq 50$ are in full agreement with the corresponding data typical for the nuclear matter. The thicknesses of transition layers in both cases are also similar and the coefficient r_0 with the factor $3^{1/3}$ included is in full correspondence with \tilde{r}_0 . The values of σ -meson mass in Table I look quite reasonable as well. However, the corresponding quantities are strongly different at small quark numbers in the droplet. We know from the experiments that

in the nuclear matter some increase of the nuclear density is observed. It becomes quite noticeable for the Helium and is much larger than the standard nuclear density for the Hydrogen.

Obviously, we understand the Thomas–Fermi approximation which is used for estimating becomes hardly justified at small number of quarks, and we should deal with the solutions of complete equation system (34). However, one very encouraging hint comes from the chiral soliton model of nucleon [28], where it has been demonstrated that solving this system (34) the good description of nucleon and Δ can be obtained. In a sense we consider an

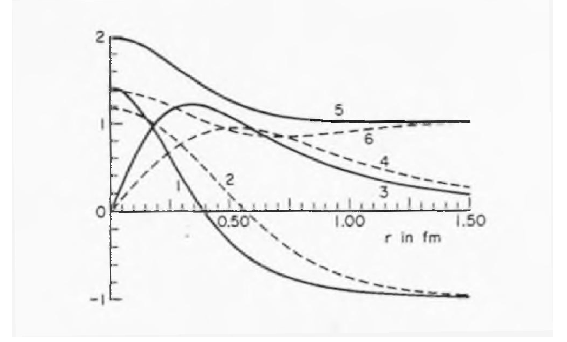


FIG. 22: The σ - and π - fields in units of F_π . Curves 1 and 2 show σ , 3 and 4 show π , 5 and 6 show $\sigma^2 + \pi^2$, (curves 1 and 3 with vector and axial-vector fields contributions included, see Ref. [28]).

analysing of just three quark system as a central result of our paper. Looking at Fig. 1 of Ref. [28] (we represent it here as Fig. 22) we see that the curve describing behavior of scalar field at large distances reaches its minimal value (according to the sign choice done in [28] it corresponds to the largest quark mass of order 300 MeV). It looks like by approaching the center of baryon a chiral symmetry is partially restored and a scalar field in the region of ~ 0.5 fm disappears. One of the possible scenario for solving the system equations (34) could be a variant in which a scalar field reaches maximal (zero) value (with a zero value of derivative over coordinat) at this (or center of baryon) point. Then a scalar field can, in principle, smoothly approach to its minimal value coming to center of baryon. It allows us conclude that we could deal with an "ordinary" quark with positive (zero) mass for the solutions of such a type. However, baryon is getting to large width (size) in this scenario. There is another type of solutions, in which a "speed" of passing by the point 0.5 fm is not getting slower. In fact such a situation could realized by doing a chiral rotation where a quark inside a baryon falls in the metastable region of negative quark masses. Such a solution develops already quite suitable width of order ~ 1 fm due to presence of massive (1 GeV) scalar field. Clearly, the problem of existence of so heavy σ -meson (strengthening the chiral effect) is crucial to collect a necessary information on a

phase diagram of strongly interacting matter. Such solutions develop the surface tension coefficient which is larger in factor two than the corresponding coefficient of single kink and as we believe signal some instability of a single kink solution.

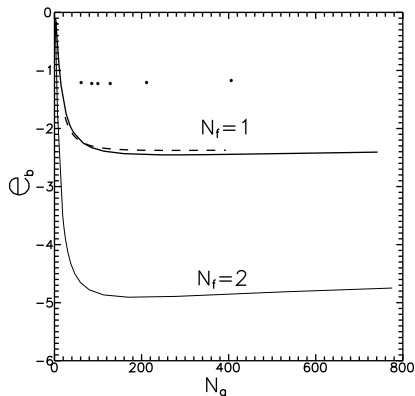


FIG. 23: The specific binding energy at $N_f = 1$ and $N_f = 2$ in MeV as a function of quark number N_q .

Fig. 23 displays the specific binding energy of ensemble. It is defined by the expression similar to Eq. (39) in that the integration over the quark droplet volume is performed. The specific energy is normalized (compared) to the ensemble energy at the spatial infinity, i.e. in vacuum. Actually, Fig. 23 shows several curves in the upper part of plot which correspond the calculations with $N_f = 1$. The solid line is obtained by scanning over parameter η and corresponds to the data presented in Table I. The dashed curve is calculated at fixed $\eta = 0.4$ but by scanning over parameter \bar{M} . It is clearly seen if the specific energy data are presented as a function of quark number N_q then the solutions, which we are interested in, rally in the local vicinity of the curve where the maximal binding energy $-|\mathcal{E}_b|$ is reached. The similar solution scanning can be performed over the central density parameter ρ_0 in origin. The corresponding data are dotted for a certain fixed \bar{M} and ρ_0 . It is interesting to notice that at scanning over any variable discussed a saturation property is observed and it looks like the minimum in e_b at $N_q \sim 200-250$. The results for the specific binding energy as a function of particle number are in the qualitative agreement with the corresponding experimental data. And one may say even about the quantitative agreement if the factor 3 (the energy necessary to remove one baryon) is taken into account. In fact, the equation system (34) represents an equation of balance for the current quarks circulating between liquid and gas phases.

Summarizing we would like to emphasize that in the

present paper we have demonstrated how a phase transition of liquid-gas kind (with the reasonable values of parameters) emerges in the NJL-type models. The constructed quark ensemble displays some interesting features for the nuclear ground state (for example, an existence of the state degenerate with the vacuum one), and the results of our study are suggestive to speculate that the quark droplets could coexist in equilibrium with vacuum under the normal conditions. These droplets manifest themselves as bearing a strong resemblance to the nuclear matter.

VI. CONCLUSION

In the present paper we described quantum liquids (Landau Fermi-liquids) resulting from the quark models with four-fermion interaction. This consideration is based on the identity of results obtained in [14] by using a dressing Bogolyubov transformation and mean field approximation. We demonstrated that the mean energy of ensemble serves as an energy functional of the Landau theory. It was shown that in a wide range of potentials interesting for applications one can expect the quantum liquids to behave in the essentially same way. For some of their properties a band of estimates was obtained. A comparison of NJL and KKB models, substantially different in many aspects, demonstrates that the properties of quantum liquids do not actually depend on a shape of the formfactor (a natural interaction length); rather, they are mainly determined by the coupling constant of interaction. It was shown that a common distinctive feature of ensembles is a presence of occupied states degenerate with respect to vacuum in chemical potential and pressure. Taking this observation the inhomogeneous states, which allowed at describing a transition layer, estimating a surface tension, as well as studying some properties of quark liquid droplets, were considered. It is noted that in the case of a small number of quarks in a droplet instability associated with lowering of the energy barrier, separating chiral phases, apparently manifests itself. This instability is seen in two kinks merging into one chiral soliton. An idea of dynamical equilibrium of a mixed phase consisting of baryon matter and vacuum was discussed as a possible scenario for explaining stability of nuclear matter.

ACKNOWLEDGMENTS

Authors are indebted D.V. Anchishkin, K. A. Bugaev, E.-M. Ilgenfritz, V.V. Skalozub, A. M. Snigirev and many other colleagues for numerous fruitful discussions. S.V.M. is deeply grateful to Professor L.V. Keldysh for interesting discussion. The work is supported by the Special Project of the Physics and Astronomy Division of the National Academy of Sciences of Ukraine.

- T. Hirano, Phys. Rev. Lett. **86** (2001) 2754;
 Phys. Rev. **C 65** (2002) 011901;
 J. Phys. **G 36** (2009) 064031.
- [2] D. Teaney, Phys. Rev. **61** (2001) 006409.
- [3] L. D. Landau, Izv. Acad. Nauk. Phys. **7** (1953) 5;
 S. Z. Belen'kii, L. D. Landau,
 Usp. Phys. Nauk. **56** (1955) 309.
- [4] K. Aamodt et al. (ALICE Collaboration)// Phys. Rev. Lett. **105** (2010) 252302
 G. Aad et al. (ATLAS Collaboration) Phys. Lett. **B707** (2012) 330.
- [5] J. Berges J., J.-P. Blaizot and F. Gelis, arXiv:1203.2042 [hep-ph].
- [6] C. P. Herzog, arXiv:0904.1975 [hep-th];
 D. Mateos, arXiv:1106.3295 [hep-th].
- [7] S. Giorgini, L. P. Pitaevskii and S. Strigari,
 Rev. Mod. Phys. **80** (2008) 1215;
 I. Bloch, J. Dalibard and W. Zwerger,
 Rev. Mod. Phys. **80** (2008) 885.
- [8] P. K. Kovtun, D. T. Son and A. D. Starinets,
 Phys. Rev. Lett. **94** (2005) 111601.
- [9] M. Mueller, J. Schmalian and I. Fritz,
 Phys. Rev. Lett. **103** (2009) 025301.
- [10] E. Shuryak and T. Sulejmanpasic, arXiv:1201.5624v3 [hep-ph].
- [11] G. M. Zinovjev and S. V. Molodtsov, Theor. Mat. Phys. **160** (2009) 444;
 S. V. Molodtsov and G. M. Zinovjev, Phys. Rev. **D80** (2009) 076001;
 S. V. Molodtsov, A. N. Sissakian and G. M. Zinovjev, Europhys. Lett. **87** (2009) 61001.
- [12] Y. Nambu and G. Jona-Lasinio, Phys. Rev. **122** (1961) 345.
- [13] L. V. Keldysh, Doctor thesis, FIAN, (1965);
 E. V. Kane, Phys. Rev. **131** (1963) 79;
 V. L. Bonch-Bruevich, in 'Physics of solid states',
 VINITI, Moscow, 1965;
 M. V. Sadovskii, Diagrammatics, World Scientific, Singapore, 2006.
- [14] S. V. Molodtsov and G. M. Zinovjev, Europhys. Lett. **93** (2011) 11001;
 S. V. Molodtsov and G. M. Zinovjev, Phys. Rev. **D84** (2011) 036011;
 G. M. Zinovjev and S. V. Molodtsov, Yad. Phys. **75** (2012) 262.
- [15] T. Hatsuda and T. Kunihiro, Phys. Rep. **247** (1994) 221.
- [16] L. D. Landau, JETP **30** (1956) 1058; **32** (1957) 59;
 D. Pines and Ph. Noziers, Theory of Quantum Liquids,
 W. A. Benjamin, New York, 1966;
 Ph. Noziers, Theory of Interacting Fermi Systems, Westview Press, Boulder, 1997;
 A. J. Leggett, Quantum Liquids, Oxford University Press, Oxford, 2006.
- [17] J. M. Luttinger and J. C. Ward, Phys. Rev. **118** (1960) 1417;
 J. M. Luttinger, Phys. Rev. **119** (1960) 1153.
- [18] H. Tezuka, Phys. Rev. **C22** (1980) 2585; **C24** (1981) 288;
 G. Baym and S. A. Chin, Nucl. Phys. **A262** (1976) 537;
 T. Matsui, Nucl. Phys. **A370** (1981) 369.
- [19] M. Asakawa and K. Yazaki, Nucl. Phys. **A504** (1989) 668.
- [20] L. Ya. Glozman, Phys. Rep. **444** (2007) 1.
- [21] G. M. Zinovjev and S. V. Molodtsov, Yad. Phys. **75** (2012) 1387;
 G. M. Zinovjev, M. K. Volkov and S. V. Molodtsov,
 Theor. Mat. Phys. **161** (2010) 408;
 S. V. Molodtsov, M. K. Volkov and G. M. Zinovjev,
 arXiv:0812.2666.
- [22] A. I. Larkin and Yu. N. Ovchinnikov, JETP **47** (1964) 1136;
 P. G. De Gennes, Superconductivity of metals and alloys,
 W. A. Benjamin, New York, 1966.
- [23] T. Eguchi and H. Sugawara, Phys. Rev. **D10** (1974) 4257;
 K. Kikkawa, Prog. Theor. Phys., **56** (1976) 947;
 M. K. Volkov, Fiz. Elem. Chast. Atom. Yadra **17** (1986) 433.
- [24] S. Carignano, D. Nickel, and M. Buballa, Phys. Rev. **D82** (2010) 054009;
 D. Nickel, Phys. Rev. Lett. **103**, (2009) 072301;
 G. Basar and G. V. Dunne, Phys. Rev. Lett. **100**, (2008) 200404;
 T. Kunihiro, Y. Minami and Z. Zhang, arXiv:1009.4534 [nucl-th];
 M. Buballa and S. Carignano, arXiv:1210.7155 [hep-ph];
 arXiv:1406.1367 [hep-ph];
 S. Carignano, M. Buballa, and B.-J. Schafer,
 arXiv:1404.0057 [hep-ph];
- [25] J. D. Walecka, Annals of Phys. **83**, (1974) 491;
 F. E. Serr and J. D. Walecka, Phys. Lett. **B79**, (1978) 10;
 N. V. Jai and L. N. Savushkin, Fiz. Elem. Chast. Atom. Yadra **23** (1992) 847.
- [26] J. Boguta and A. Bodmer, Nucl. Phys. **A292**, (1977) 413;
 M. B. Pinto, V. Koch and J. Randrup, Phys. Rev. **C86** (2012) 025203; arXiv:1207.5186 [hep-ph];
 J. J. Bjerrum-Bohr, I. N. Mishustin and T. Dossing
 arXiv:1112.2514 [nucl-th];
 N. Itoh, Prog. Theor. Phys. **44** (1970) 291;
 P. W. Anderson, N. Itoh, Nature **256** (1975) 25.
- [27] K. Huang and D. R. Stump, Phys. Rev. **D14**, (1976) 223;
 R. Friedberg and T. D. Lee,
 Phys. Rev. **D18**, (1978) 2623;
 R. Goldflam and L. Wilets, Phys. Rev. **D25**, (1982) 1951;
 E. G. Lübeck, M. C. Birse, E. M. Henley, and L. Wilets,
 Phys. Rev. **D33**, (1986) 234.
- [28] W. Broniowski and M. K. Banerjee, Phys. Lett. **B158** (1978) 335.
- [29] Generally speaking, in such a correlation function the terms spanned on the vector of relative distance are allowed, but for simplicity we ignore them.
- [30] It is obvious that we are telling about an approximate calculation of corresponding generating functional for some specific conditions with the restricted area of applicability that does not imply the calculation of functional derivatives of arbitrary order.
- [31] In the KKB model the fermion behavior is considered in the stochastic random field with infinite correlation length (the NJL model corresponds to the 'white noise' with zero correlation length). In this case one is lucky enough to be able to 'sum up' an entire diverging series and, therefore, to demonstrate that fermions are in general not on mass shell.
- [32] If one decides to take the dynamical quark mass M_q , as a basic variable, then it is seen from Eq.(9) that formulating an inverse transformation from M_q to \widetilde{M} suitable for handling is difficult.